Published April 14, 2008

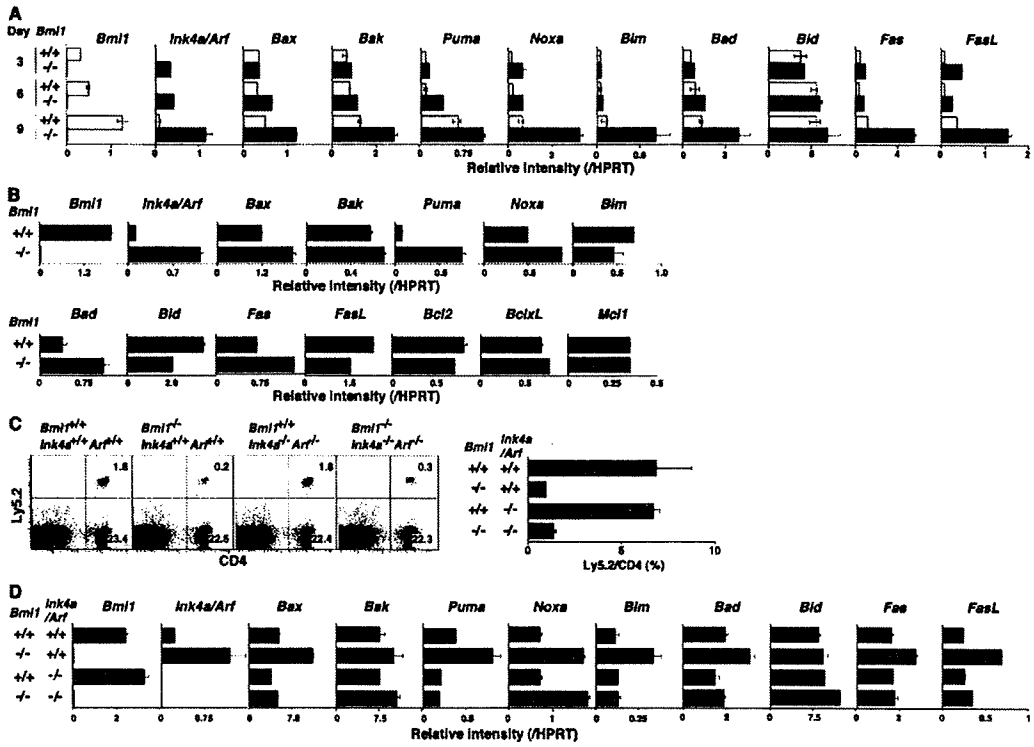

Figure 2. Deletion of the *p16*^{Ink4a} and *p19*^{Arf} genes failed to rescue the impaired generation of memory Th2 cells in the absence of Bmi1. (A) mRNA expression of *Ink4a/Arf* and p53-related proapoptotic genes in *Bmi1*$^{-/-}$ effector Th2 cells was determined by quantitative RT-PCR. The relative intensity (/HPRT; mean of three samples) is shown with standard deviations. Three independent experiments were performed with similar results. (B) mRNA expression of *Ink4a/Arf*, p53-related proapoptotic genes, and antiapoptotic genes in *Bmi1*$^{-/-}$ memory Th2 cells was analyzed. The relative intensity (/HPRT; mean of three samples) is shown with standard deviations. Two independent experiments were performed with similar results. (C) Effects on p16^{Ink4a} and p19^{Arf} deficiency on the memory Th2 cell generation. The effector Th2 cells from the indicated mice (Ly5.2 background) were transferred into Ly5.1 host mice. 5 wk after cell transfer, the number of Ly5.2$^+$ memory Th2 cells was determined. The mean values are shown with standard deviations ($n = 5$; right). The experiments were performed twice with similar results. (D) mRNA levels of proapoptotic genes in *Bmi1*$^{-/-}$/*Ink4a*$^{-/-}$/*Arf*$^{-/-}$ effector Th2 cells were determined by quantitative RT-PCR. The relative intensity (/HPRT; mean of three samples) is shown with standard deviations. The experiments were performed twice with similar results.

restore memory Th2 cell generation in *Bmi1*$^{-/-}$ background (Fig. 2 C, panels 2 and 4). Furthermore, the deletion of the p53 gene failed to rescue the *Bmi1*$^{+/-}$ memory Th2 cell numbers (Fig. S6, available at http://www.jem.org/cgi/content/full/jem.20072000/DC1). These results suggest that the Ink4/Arf and p53-dependent pathways are not key pathways responsible for the reduced memory Th2 cell generation in *Bmi1*$^{-/-}$ memory mice. To identify any possible proapoptotic genes whose expression is regulated by Bmi1 but not regulated by the Ink4/Arf and p53-dependent pathways, the expression levels of these proapoptotic genes were assessed in the *Bmi1*$^{-/-}$/*Ink4a*$^{-/-}$/*Arf*$^{-/-}$ Th2 cells. Among these proapoptotic genes, the level of *Noxa* mRNA increased in *Bmi1*$^{-/-}$ Th2 cells and remained high in *Bmi1*$^{-/-}$/*Ink4a*$^{-/-}$/*Arf*$^{-/-}$ background, whereas other targets such as *Bax*, *Puma*, *Bim*, *Bad*, *Fas*, and *Fas ligand* were at the normal expression levels (Fig. 2 D). Increased expression of *Noxa* mRNA was observed also in effector Th1, Tc1, and Tc2 cells in the absence of Bmi1 (Fig. S7). These results indicate that the expression of *Noxa* is suppressed by the expression of Bmi1, but it is independent from the control of the Ink4/Arf and p53 pathways. The results thus far obtained suggest that Bmi1 controls the generation of both Th1 and Th2 memory cells accompanied with an increased expression of Noxa. Our previous study indicated that the expression of Bmi1 is higher in Th2 cells than Th1 cells, and Bmi1 controls the generation of Th2 cells more profoundly as compared with Th1 cells (33). Therefore, to better understand the molecular mechanisms underlying the Bmi1/Noxa-mediated regulation of memory CD4 T cell generation, we focused much of our studies on memory Th2 cells.

The expression of Noxa controls the generation of memory Th2 cells

Consequently, to test whether the changes in the level of Noxa affect the induction of cell death, effector Th2 cells were infected with a retrovirus containing the human *NGFR* and *Noxa*, and the number of annexin V$^+$ cells was assessed

Published April 14, 2008

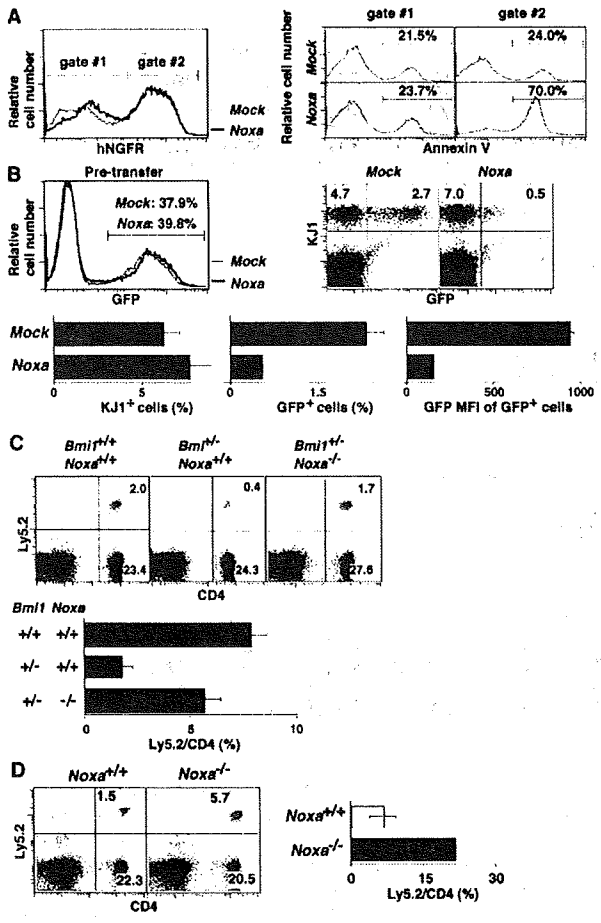

Figure 3. Expression level of Noxa controls the generation of memory Th2 cells. (A) Enforced expression of Noxa-induced cell death in effector Th2 cells after cytokine depletion. Effector Th2 cells infected with a *Noxa-IRES-hNGFR*-containing retrovirus were cultured in vitro for 24 h without cytokines. hNGFR profiles (left) and annexin V staining profiles of the electronically gated hNGFR$^+$ (gate #2) and hNGFR$^-$ (gate #1) populations are shown. Three independent experiments were performed with similar results. (B) KJ1$^+$ effector Th2 cells infected with *Noxa-IRES-EGFP*-containing retrovirus were transferred into BALB/c *nu/nu* mice. 5 wk later, memory Th2 cell generation was determined by KJ1/EGFP expression. Expression of EGFP in pretransferred effector Th2 cells (top left) and a typical KJ1/GFP profile of freshly prepared memory Th2 cells (top right) are shown. In the bottom panels, the percentages of KJ1$^+$ cells and GFP$^+$ Noxa-overexpressing cells and the mean fluorescence intensity of the GFP$^+$ cells are shown with standard deviations ($n = 4$). The experiments were performed twice with similar results. (C) The effector Th2 cells from *Bmi1*$^{+/+}$/*Noxa*$^{+/+}$, *Bmi1*$^{+/-}$/*Noxa*$^{+/+}$, and *Bmi1*$^{+/-}$/*Noxa*$^{-/-}$ mice (Ly5.2) were transferred into Ly5.1 host mice, and the number of Ly5.2$^+$ memory Th2 cells was determined. A typical staining pattern of CD4/Ly5.2 (top) and the percentages of Ly5.2$^+$ cells among CD4 T cells are shown with standard deviations ($n = 5$; bottom). Three independent experiments were performed with similar results. (D) Deletion of the *Noxa* gene enhanced the generation of memory Th2 cells. In vitro-generated *Noxa*$^{-/-}$ effector Th2 cells (Ly5.2) were transferred into Ly5.1 host mice. 5 wk after cell transfer, the number of Ly5.2$^+$ memory Th2 cells was determined. A representative CD4/Ly5.2 profile (left) and the mean values with standard deviations ($n = 5$; right) are shown. The experiments were performed twice with similar results.

after in vitro suspension culture for 24 h without cytokines. *Noxa*-introduced cells showed increased annexin V$^+$ staining (70.0%) as compared with mock-infected (24.0%) or noninfected cell populations (Fig. 3 A). Next, KJ1$^+$ effector Th2 cells infected with a retrovirus containing the *GFP* and *Noxa* genes were transferred into BALB/c *nu/nu* mice, and the numbers of Noxa-expressing (KJ1$^+$GFP$^+$) memory Th2 cells were assessed. Although the generation of KJ1$^+$ memory Th2 cells was not affected, the number of KJ1$^+$GFP$^+$ memory Th2 cells and their GFP mean fluorescence intensity were clearly reduced in the Noxa-transduced group (Fig. 3 B). A gene dose-dependent increase in the expression of Noxa was detected in *Bmi1*$^{+/-}$ and *Bmi1*$^{-/-}$ memory Th2 cells (Fig. S8, available at http://www.jem.org/cgi/content/full/jem.20072000/DC1). *Bmi1*$^{-/-}$*Noxa*$^{-/-}$ mice were not born despite extensive breeding attempts. Consequently, we used *Bmi1*$^{+/-}$*Noxa*$^{-/-}$ mice and found that memory Th2 cell generation in the mice transferred with *Bmi1*$^{+/-}$ effector Th2 cells was restored by the deletion of the *Noxa* gene (Fig. 3 C). Furthermore, enhanced generation of memory Th2 cells was observed in the mice that received Noxa$^{-/-}$ effector Th2 cells (Fig. 3 D). Thus, we concluded that the reduction in the number of *Bmi1*$^{-/-}$ memory Th2 cells is at least in part due to the increased expression of Noxa in *Bmi1*$^{-/-}$ Th2 cells.

Bmi1 directly binds to the *Noxa* gene locus and regulates the histone modification

To assess the molecular mechanisms underlying the Bmi1-mediated repression of the *Noxa* gene, we performed chromatin immunoprecipitation (ChIP) assays with six primer pairs covering the *Noxa* gene (Fig. 4 A). The accumulation of Bmi1 was observed around the CpG island (Fig. 4 B, #2 and #3) of the *Noxa* locus. The binding of Bmi1 was confirmed by a ChIP assay with a quantitative PCR system (Fig. 4 C). Equivalent binding of Bmi1 was observed in Th1 cells (Fig. S9, available at http://www.jem.org/cgi/content/full/jem.20072000/DC1). Histone H3-K9/14 acetylation and tri-methylation of histone H3-K4 were observed also around the CpG island (Fig. 4 D, #2 and #3). More interestingly, histone H3-K27 was highly tri-methylated in wild-type Th2 cells over broader regions in the Noxa locus, and the tri-methylation was apparently reduced in the *Bmi1*$^{-/-}$ Th2 cells (Fig. 4 D). The changes in histone modifications were also assessed using a quantitative PCR system. Modest increase in histone H3-K9/14 acetylation and a substantial decrease in H3-K27 tri-methylation at the *Noxa* gene locus were confirmed in the *Bmi1*$^{-/-}$ Th2 cells (Fig. 4 E) and *Bmi1*$^{-/-}$ Th1 cells (Fig. S10). Interestingly, the levels of histone H3-K27 tri-methylation at the *Ink4a* gene locus, another target gene of Bmi1, were not affected by the depletion of *Bmi1* (Fig. 4 E). The levels of histone H3-K27 tri-methylation at the promoter regions of the

Published April 14, 2008

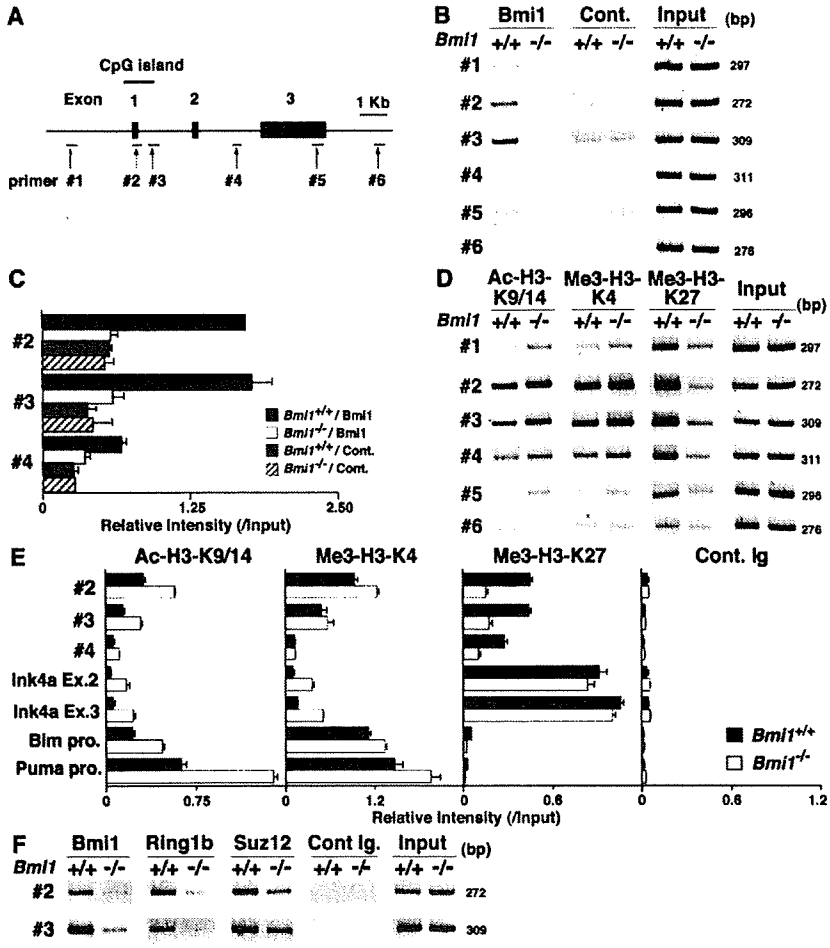

Figure 4. Bmi1 binds to the *Noxa* gene and regulates tri-methylation of H3-K27. (A) Schematic representation of the *Noxa* gene locus. The location of primers (#1 to #6), a CpG island, and exons are indicated. (B) A ChIP assay of the *Noxa* gene locus was performed using anti-Bmi1 antibody (Bmi1) and control antibody (Cont.) in *Bmi1*$^{+/+}$ and *Bmi1*$^{-/-}$ Th2 cells. Three independent experiments were performed with similar results. (C) A ChIP assay of the *Noxa* gene locus was performed as in B, and the levels of binding were assessed by a quantitative PCR analysis. (D) Histone modifications (Ac-H3-K9/K14; acetylation of histone H3-K9/K14 and Me3-H3-K4; tri-methylation of histone H3-K4 and Me3-H3-K27; tri-methylation of histone H3-K27) at the *Noxa* gene locus in *Bmi1*$^{+/+}$ and *Bmi1*$^{-/-}$ effector Th2 cells. (E) A ChIP assay of the *Noxa* (#2 to #4), *Ink4a* (Ex.2, exon 2; Ex.3, exon 3), *Bim* (Bim pro., *Bim* promoter), and *Puma* (Puma pro., *Puma* promoter) locus was performed as in D, and the levels of binding were assessed by a quantitative PCR analysis. (F) The association of Ring1B and Suz12 at the *Noxa* gene locus in *Bmi1*$^{+/+}$ and *Bmi1*$^{-/-}$ Th2 cells. The association of Bmi1, Ring1B, and Suz12 was determined by a ChIP assay using specific antibodies.

Bim and *Puma* were not significantly detected in the presence or absence of Bmi1. The binding of other PcG gene products, such as Ring1b and Suz12, was detected around the same regions (Fig. 4 F, #2 and #3), and the binding was substantially decreased in the absence of Bmi1. Thus, a PcG gene product complex containing Bmi1 appears to bind to the *Noxa* gene directly and regulate histone modifications, such as tri-methylation of H3-K27 in Th1 and Th2 cells.

Bmi1 controls the CpG methylation at the *Noxa* gene locus and represses the mRNA expression of *Noxa*

Next, to study the levels of CpG DNA methylation around the CpG island of the *Noxa* gene, a methylated DNA immunoprecipitation (MeDIP) assay was performed. As shown in Fig. 5 A, the 5′ region of the CpG island (promoter and #2) was methylated in wild-type effector Th2 cells, and the methylation levels were very low in the *Bmi1*$^{-/-}$ cells. A DNA methyltransferase Dnmt1 was found to bind at the CpG island (Fig. 5 B, #2 and #3), and the binding was also dependent on Bmi1 in Th2 cells (Fig. 5 B) and Th1 cells (Fig. S11, available at http://www.jem.org/cgi/content/full/jem.20072000/DC1). To assess a role of CpG methylation on Noxa expression, effector Th2 cells were treated with 5-Aza-2′-deoxycytidine (5-Aza), an inhibitor of CpG DNA methylation. As expected, the expression of *Noxa* mRNA was dramatically increased (Fig. 5 C) accompanied by the reduction of a tri-methylation

Published April 14, 2008

level of histone H3-K27 (Fig. S12). Furthermore, the binding of Bmi1, Ring1b, and Suz12 was substantially reduced by the treatment with 5-Aza (Fig. 5 D). A similar increase in the expression of *Noxa* and the 5-Aza–dependent reduction in the binding of Bmi1 were observed in Th1 cells (Fig. S13). Finally, we established a knockdown system for Dnmt1 using a cultured T cell line, TG40, as described in Materials and methods. Up-regulation of *Noxa* mRNA (Fig. 5 E) and the reduction of Bmi1 binding at the Noxa gene locus (Fig. 5 F) were induced by the introduction of shRNA for Dnmt1. Enhanced *Noxa* mRNA expression was induced in primary Th2 cells by the treatment with a DNA methyltransferase inhibitor, RG108 (Fig. S14). These results indicate that a DNA methyltransferase Dnmt1 plays an important role in the recruitment of PcG gene products and the expression of the *Noxa* gene in Th2 cells.

The expression of Bmi1 is required for memory Th2 cell–dependent immune responses and inflammation in vivo

Finally, to examine functional defects in $Bmi1^{-/-}$ memory Th2 mice, we used a memory Th2 cell–dependent allergic airway inflammation model (36). Memory Th2 mice were generated and simply challenged by inhalation with OVA four times. The OVA-specific IgE and IgG1 (Th2-dependent isotypes) antibody production were decreased in the $Bmi1^{-/-}$ memory Th2 mice, whereas only a marginal decrease in the levels of Th1-dependent IgG2a was seen (Fig. 6 A). Next, we examined the levels of airway inflammation after OVA inhalation. The extent of inflammatory leukocyte infiltration in the peri-bronchiolar region (Fig. 6 B) and the infiltrated eosinophils, lymphocytes, and macrophages in the bronchioalveolar lavage (BAL) fluid (Fig. 6 C) was reduced significantly in the $Bmi1^{-/-}$ memory Th2 mice as compared with wild-type mice. The expression of Th2 cytokines (IL-4, IL-5, and IL-13) and Eotaxin 2 in the lung of OVA-inhaled $Bmi1^{-/-}$ memory Th2 mice was also reduced (Fig. 6 D). The periodic-acid-Schiff staining and the measurement of mRNA expression of *Gob5*, *Muc5a/c*, and *Muc5b* in the lung indicated a decrease in mucus hyperproduction in $Bmi1^{-/-}$ memory Th2 mice (Fig. 7, A and B). Furthermore, the airway hyperresponsiveness measured using a whole-body plethysmograph was not significantly induced in the $Bmi1^{-/-}$ memory Th2 mice (Fig. 7 C). In addition, by a direct invasive assay for lung resistance (RL), increase in the RL and decrease in the dynamic compliance were observed in the $Bmi1^{-/-}$ memory Th2 mice (Fig. 7 D). Collectively, these results indicate that the memory Th2 cell–dependent allergic responses were thus compromised in the $Bmi1^{-/-}$ memory Th2 mice. We also assessed the eosinophilic infiltration in DO11.10 Tg $Bmi1^{+/+}$ and $Bmi1^{+/-}$ mice without cell transfer, and as expected, the level of eosinophilic infiltration was significantly milder in the $Bmi1^{+/-}$ mice (not depicted).

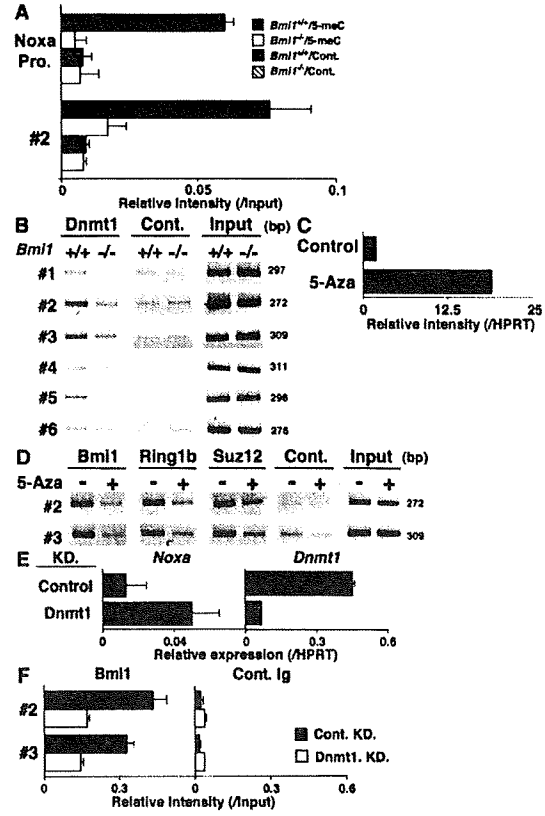

Figure 5. Bmi1 is required for the DNA CpG methylation of the Noxa gene. (A) Decreased DNA CpG methylation at the CpG island of the *Noxa* gene locus in $Bmi1^{-/-}$ Th2 cells. DNA CpG methylation level was determined by MeDIP assay. MeDIP assay was performed using an anti-5-methyl cytidine antibody (5-meC) and a control antibody (Cont.). Mean values with standard deviation are shown ($n = 3$). (B) The association of Dnmt1, a DNA methyltransferase, at the CpG island of the *Noxa* gene locus. The association of Dnmt1 was determined by a ChIP assay using a specific antibody. (C) Increased mRNA expression of *Noxa* after the treatment with 5-Aza, an inhibitor of DNA methyltransferase. Th2 cells were treated with 5-Aza for 2 d, and *Noxa* mRNA expression was determined by a quantitative RT-PCR system. Three independent experiments were performed with similar results. (D) Dissociation of the PcG complex from the *Noxa* gene locus after the treatment with 5-Aza. The association of Bmi1, Ring1B, and Suz12 was determined by a ChIP assay using specific antibodies. Three independent experiments were performed with similar results. (E) mRNA expression of *Noxa* and *Dnmt1* in a Dnmt1 knockdown (KD) T cell line. Dnmt1-KD and control-KD stable TG40 cell lines were generated using a lentivirus gene transduction system as described in Materials and methods. The levels of mRNA were determined by a quantitative RT-PCR. The relative intensity (/HPRT; mean of three samples) is shown with standard deviations. (F) Decreased binding of Bmi1 at the *Noxa* gene in Dnmt1-KD TG40 cells. A ChIP assay with an anti-Bmi1 antibody was performed, and the levels of Bmi1 binding were assessed by a quantitative PCR analysis.

DISCUSSION

Here, we demonstrate that Bmi1 plays a crucial role in the generation and maintenance of memory CD4 T cells. Such a Bmi1-mediated regulation was seen in both memory Th1 and Th2 cells. In the absence of Bmi1, the generation of both Th1 and Th2 memory cells was impaired (Fig. 1 and Fig. S2)

Published April 14, 2008

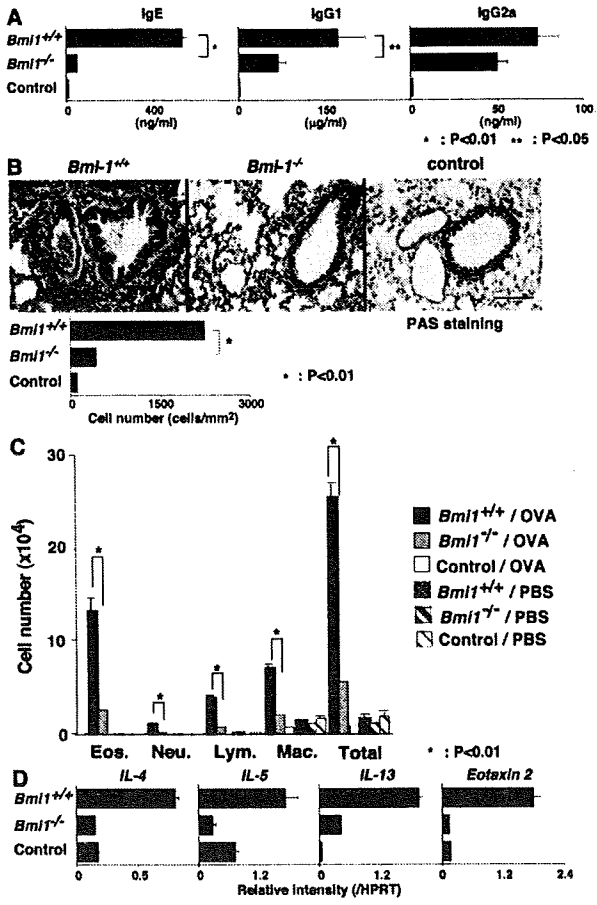

Figure 6. Defects in the memory Th2 cell-dependent immune responses and inflammation in *Bmi1*$^{-/-}$ memory Th2 mice. OVA-specific *Bmi1*$^{+/+}$ and *Bmi1*$^{-/-}$ effector Th2 cells with DO11. 10 Tg background were intravenously transferred into BALB/c *nu/nu* mice. 5 wk later, the mice were challenged four times by inhalation with OVA on days 0, 2, 8, and 10. (A) The serum concentrations of OVA-specific Igs with the indicated isotype after OVA inhalation (on day 11) were determined by ELISA. The mean values with standard deviations (five animals per group) are shown. *, $P < 0.01$; **, $P < 0.05$. The control represents BALB/c *nu/nu* mice without Th2 cell transfer. The experiments were performed twice with similar results. (B) On day 11, the lungs were fixed and stained with hematoxylin an eosin (HE). The number of infiltrated leukocytes in the peribronchiolar region (mean cell numbers/mm^2 with standard deviations; $n = 5$) is also shown (bottom). The experiments were performed twice with similar results. Bars, 100 μm. (C) On day 12, BAL fluid was collected and May-Grunwald-Giemsa staining was performed. The absolute cell numbers of eosinophils (Eos.), neutrophils (Neu.), lymphocytes (Lym.), and macrophages (Mac.) in the BAL fluid are shown with standard deviations ($n = 5$). The results were obtained using the values of cell counting, the percentage of the cells, the total cell number per milliliter, and the volume of the BAL fluid recovered. *, $P < 0.01$. The experiments were performed twice with similar results. (D) The mRNA expression of *IL-4*, *IL-5*, *IL-13*, and *Eotaxin 2* was determined by quantitative RT-PCR. The relative intensity (/HPRT; mean of three samples) is shown with standard deviations. The experiments were performed twice with similar results.

by the increased Noxa expression (Fig. 2 and Fig. S7). Bmi1 binds to the *Noxa* gene locus in both Th1 and Th2 cells (Fig. 4 and Fig. S9), and directly represses its transcription to promote memory Th2 cell survival. The involvement of H3-K27 tri-methylation and DNA CpG methylation in the repression of *Noxa* was revealed. The Th2-dependent allergic airway inflammatory responses were compromised in *Bmi1*$^{-/-}$ memory Th2 mice, suggesting a physiological role of Bmi1 in the establishment of Th2 cell–mediated memory responses.

Noxa is a member of a BH3-only protein family that initiates programmed cell death in various cells, including lymphocytes (39–41). Noxa is known to regulate selectively the pro-survival activity of Mcl1 and A1/Bfl-1 (42), and an important role of Mcl1 in the survival of lymphocytes was reported (43). The mRNA expression of antiapoptotic genes Mcl1, Bclx, and BclxL was not changed in *Bmi1*$^{-/-}$ memory (Fig. 2 B) and induced normally in effector Th2 cells by the IL-7 treatment (unpublished data). Enforced expression of Noxa in effector Th2 cells resulted in the decreased generation of memory Th2 cells (Fig. 3 B), suggesting that the overproduction of Noxa prevents memory Th2 cell generation even in the presence of normal abundance of antiapoptotic proteins. Thus, it is likely that Bmi1 attenuates Noxa-mediated inhibition of Mcl1 pro-survival activity and promotes memory T cell generation.

Noxa was originally identified as a downstream target of p53 (44). Arf/Mdm2-mediated stabilization of p53 protein and the resulting mRNA expression of the p53 target genes were reported (45, 46). Therefore, it was likely that the enhancement of cell death observed in *Bmi1*$^{-/-}$ Th2 cells is p53 dependent. However, the deletion of the *p53* gene failed to rescue the decreased generation of memory Th2 cells in the absence of Bmi1 (Fig. S6). Thus, an increased apoptotic cell death observed in *Bmi1*$^{-/-}$ memory Th2 cells appears to be p53 independent.

The Bmi1-mediated repression of the *Ink4a/Arf* gene observed in the hematopoietic and neural stem cells (45, 46) appears to operate in Th2 cells (Fig. 2, A and B). It is known that Arf induces p53 activation (38), resulting in the induction of p53-dependent genes, including Puma and Bim. An important role of Puma and Bim in the cell death of activated T cells was reported (47, 48), and the expression of these genes was up-regulated in *Bmi1*$^{-/-}$ effector and memory Th2 cells (Fig. 2, A and B). However, *Bmi1*$^{-/-}$/*Ink4a*$^{-/-}$/*Arf*$^{-/-}$ Th2 cells, in which the levels of Puma and Bim expression were not increased (Fig. 2 D), failed to generate normal numbers of memory Th2 cells (Fig. 2 C). Although the expression of *Puma* and *Bim* mRNA was up-regulated, the levels were considerably low compared with Noxa in *Bmi1*$^{-/-}$ effector Th2 cells (Fig. 2 A). This might explain the predominant effect of Noxa in the cell death of *Bmi1*$^{-/-}$ Th2 cells. However, the current experimental data do not allow us to make any conclusions to be drawn in regards to the relative contribution of each of the factors in the survival of CD4 T cells. Thus, although Puma and Bim may play a role in the survival of memory Th2 cells, Noxa appears to be a

Published April 14, 2008

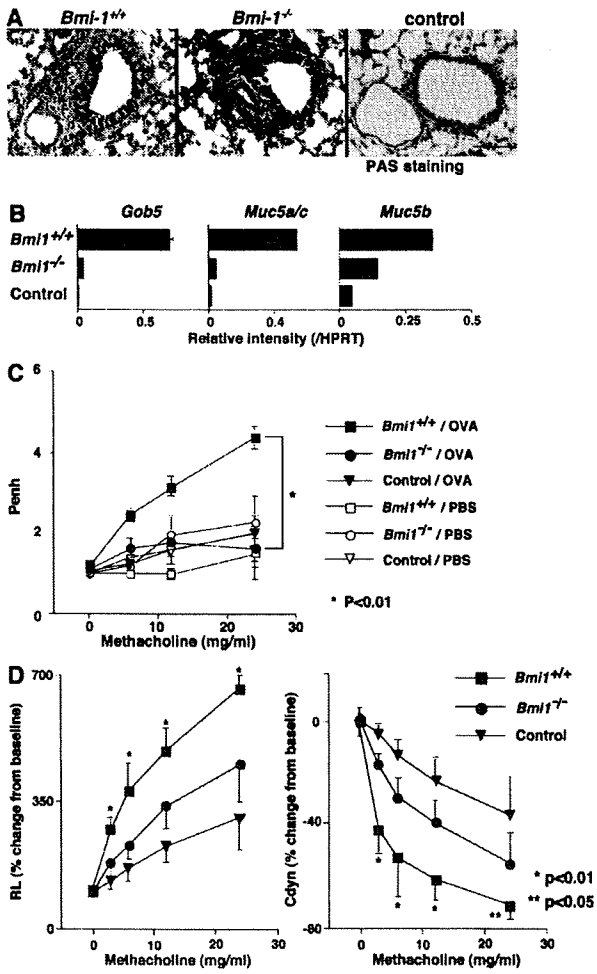

Figure 7. Decreased mucus hyperproduction and airway hyperresponsiveness in *Bmi1*$^{-/-}$ memory Th2 mice. *Bmi1*$^{+/+}$ and *Bmi1*$^{-/-}$ memory Th2 mice were challenged by inhalation with OVA as in Fig. 5. (A) 1 d after the last OVA inhalation (day 11), the lungs were fixed and stained with periodic-acid-Schiff (PAS). A representative staining pattern is shown. The control represents BALB/c *nu/nu* mice without Th2 cell transfer. Bars, 100 µm. (B) On day 12, total RNA was prepared from the lung, and the expression of *Gob5*, *Muc5a/c*, and *Muc 5b* (molecular makers for Goblet cell hyperplasia and mucus production) was determined by a quantitative PCR analysis. The relative intensity (/HPRT; mean of three samples) is shown with standard deviations. (C) OVA-induced airway hyperresponsiveness in *Bmi1*$^{-/-}$ memory Th2 mice. On day 11, the airway hyperresponsiveness in response to increasing doses of methacholine was measured in a whole-body plethysmograph. The mean values ($n = 5$) are shown with standard deviations. PBS, PBS-inhaled control; OVA, OVA-inhaled. *, $P < 0.01$. The experiments were performed twice with similar results. (D) On day 11, changes in the RL (left) and the dynamic compliance (Cdyn; right) were assessed. Mean values (six mice per group) are shown with standard deviations. *, $P < 0.01$; **, $P < 0.05$.

critical target for the Bmi1-mediated regulation of memory Th2 cell survival.

Semi-acute survival of transferred *Bmi1*$^{-/-}$ effector Th2 cells was substantially impaired (Fig. 1 D and Figs. S3–S5). On the other hand, high numbers of apoptotic cells were detected in the spleen even 5 wk after effector *Bmi1*$^{-/-}$ Th2 cell transfer (Fig. 1 F). The extent of the defect in homeostatic proliferation was modest (Fig. 1 E). The low number of *Bmi1*$^{-/-}$ memory CD4 T cells persisted for at least 2 mo (unpublished data). These results suggest that the long-term survival of memory Th2 cells is also dependent on the expression of Bmi1. Collectively, we conclude that Bmi1 controls both semi-acute survival of effector Th2 cells and long-term survival of memory Th2 cells.

The PRC2 was reported to possess an intrinsic histone H3-K27 methyltransferase activity (26–29). The PRC1, including Bmi1 and Ring1, was shown to possess an activity of histone H2A ubiquitination (49–51), whereas there has been no report indicating that the PRC1 possess an intrinsic histone H3-K27 methyltransferase activity. Accumulating evidence supports a sequential binding model (52), in which PRC2-mediated H3-K27 methylation serves as a binding site for the recruitment of PRC1 complex through the specific recognition of the H3-K27 methyl mark by the chromo domain of the polycomb protein, such as M33 (53, 54). In our study, however, the levels of tri-methylation of histone H3-K27 were substantially decreased in *Bmi1*$^{-/-}$ Th1 and Th2 cells (Fig. S10 and Fig. 4, D and E). In addition, the levels of binding of Suz12, a component of PRC2, at the *Noxa* gene locus were decreased in *Bmi1*$^{-/-}$ Th2 cells (Fig. 4 F). Thus, in Th2 cells, Bmi1 may play an important role for the recruitment of PRC2 and subsequent histone H3-K27 methylation at the Noxa gene locus. Alternatively, the Bmi1-containing PcG complex in Th2 cells may associate with a unique molecule possessing an intrinsic histone H3-K27 methyltransferase activity. In any event, tri-methylation of histone H3-K27 at the Noxa gene locus is strictly regulated by the expression of Bmi1.

The expression of Bmi1 is required for the DNA CpG methylation of the *Noxa* gene (Fig. 5 A). The binding of Dnmt1 at the CpG island was Bmi1 dependent (Fig. 5 B and Fig. S11). The treatment with a 5-Aza resulted in the dissociation of Bmi1, Ring1B, and Suz12 from the CpG island (Fig. 5 D) and the up-regulation of Noxa mRNA (Fig. 5 C and Fig. S13 A). Increased expression of Noxa mRNA and reduced binding of Bmi1 were confirmed in Dnmt1 knockdown T cells (Fig. 5, E and F). Recently, the PcG complex was reported to be associated with DNA methyltransferases, including Dnmt1 (55, 56). Thus, a DNA methyltransferase, such as Dnmt1, may play a critical role in the recruitment and the repressive function of the PcG complex at the *Noxa* gene.

In this study, we demonstrate that the generation and maintenance of memory Th1/Th2 cells (Fig. 1) and the memory Th2 cell–dependent airway inflammation are controlled by the expression of Bmi1 (Figs. 6 and 7). Our preliminary experiments demonstrate that at least Mel-18, Mph1/Rae28, and M33 appear to be involved in the regulation of memory Th2 cell generation (unpublished data), suggesting that the survival of memory Th2 cells is regulated by an epigenetic mechanism involving the Bmi1-containing PcG complex. We have recently reported that Bmi1 stabilizes GATA3 protein

Published April 14, 2008

through the direct interaction with GATA3 (33). Mel-18 is involved in the induction of GATA3 expression in developing Th2 cells (32). Collectively, PcG gene products appear to control the development of effector and memory Th2 cells at multiple steps in a distinct manner and govern the Th2-type immune responses and inflammation.

MATERIALS AND METHODS

Mice. Bmi1-deficient mice were provided by M. van Lohuizen (The Netherlands Cancer Institute, Amsterdam, Netherlands) (30). $p16^{Ink4a}/p19^{Arf}$ double-deficient mice were provided by R.A. DePinho (Harvard Medical School, Boston, MA) (37). Noxa-deficient mice were provided by T. Taniguchi (The University of Tokyo, Tokyo, Japan) (44). The animals used in this study were backcrossed to BALB/c or C57BL/6 mice 10 times. Anti–OVA-specific TCR-αβ (DO11.10) Tg mice were provided by D. Loh (Washington University School of Medicine, St. Louis, MO) (57). All mice were used at 4–8 wk old. BALB/c and BALB/c *nu/nu* mice were purchased from Clea Inc. Ly5.1 mice were purchased from Sankyo Laboratory. All mice used in this study were maintained under specific pathogen-free conditions. All experiments using mice received approval from the Chiba University Administrative Panel for Animal Care. Animal care was conducted in accordance with the guidelines of Chiba University.

Reagents. The reagents used in this study are as follows: FITC- or APC-conjugated anti-CD4 mAb (GK1.5), FITC-conjugated anti-Ly5.2 mAb (104), and PE-conjugated KJ1 (anti-clonotypic mAb for DO11.10 TCR) were purchased from BD Biosciences. Anti-FcRγII and III mAb (2.4G2) and unconjugated anti–IL-4 mAb (11B11), anti–IL-12 mAb (C17.8), and anti–IFN-γ (R4-6A2) were used as culture supernatants. Recombinant mouse IL-4 was from TOYOBO. The OVA peptide (residues 323–339; ISQAVHAAHAEINEAGR) was synthesized by BEX Corporation.

The generation of effector and memory Th1/Th2 cells. Effector and memory Th1/Th2 cells were generated as described previously (35, 36). In brief, splenic $KJ1^+CD4^+$ T cells from DO11.10 OVA-specific TCR Tg mice were stimulated with 1 μM of an OVA peptide (Loh15) plus APC (irradiated splenocytes) under the Th1 or Th2 culture conditions for 6 d in vitro. Th1 condition: 25 U/ml IL-2, 10 U/ml IL-12, and anti–IL-4 mAb. Th2 condition: 25 U/ml IL-2, 10 U/ml IL-4, anti–IL-12 mAb, and anti–IFN-γ mAb. In some experiments, splenic CD4 T cells were stimulated with 3 μg/ml of immobilized anti–TCR-β mAb plus 1 μg/ml anti-CD28 mAb. These effector Th1/Th2 cells (3×10^7) were transferred intravenously into BALB/c *nu/nu*, BALB/c, or Ly5.1 C57BL/6 recipient mice. 5 wk after cell transfer, the generation of memory Th2 cells was assessed using donor cell–specific mAbs (KJ1 and anti-Ly5.2).

TUNEL assay. TUNEL assay was performed with In Situ Cell Detection kit (Roche).

Measurement of BrdU incorporation in vivo. The memory Th2 mice were treated twice with 1 mg BrdU on days 0 and 2. BrdU incorporation in splenic $KJ1^+$ memory Th2 cells was assessed on day 4 using the BrdU Flow kit (BD Biosciences).

5-Aza treatment. Developing Th2 cells were treated with 10 μM 5-Aza (Sigma-Aldrich) for 3 d, and then total RNA was prepared.

ELISA. Serum OVA–specific Ig concentrations were determined by ELISA as described previously (36).

Quantitative RT-PCR. Total RNA was isolated using the TRIzol reagent (Invitrogen). cDNA was synthesized using oligo (dT) primer and Superscript II RT (Invitrogen). Quantitative RT-PCR was performed as described previously using ABI PRISM 7000 Sequence Detection System (36). The primers for TaqMan probes for the detection were purchased from Applied Biosystems. The expression was normalized using the HPRT signal.

Retrovirus infection. Retrovirus vector, pMXs-IRES-GFP, was provided by T. Kitamura (The University of Tokyo, Tokyo, Japan). The method for the generation of virus supernatant and the infection was described previously (32). Infected cells were collected 4 d after infection and transferred into recipient mice.

Lentivirus infection. Lentivirus vectors, pLKO.1 (SHC002) and pLKO.1 mouse Dnmt1 (TRCN39024), were purchased from Sigma-Aldrich. pCAG-HIVgp and pCMV-VSV-G-RSV-Rev vectors were provided by H. Miyoshi (RIKEN Bioresource Center, Ibaraki Japan). Recombinant lentiviruses were generated using a three-plasmid system as described previously (58). In brief, 293 T cells were transfected with self-inactivating lentiviral vector, pCAG-HIVgp vector, and pCMV-VSV-G-RSV-Rev vector. Virus containing culture supernatant was collected 48 h after transfection and used for infection. T cell line TG40 (2.5×10^5/well) was infected and selected using puromycin.

ChIP assay. ChIP assay was performed as described previously (59). The antibodies using ChIP assay are as follows; anti-trimethyl histone H3-K4 (ab8580; Abcam), anti-trimethyl histone H3-K9 (Abcam), anti-trimethyl histone H3-K27 (Millipore), anti-Bmi1 (Santa Cruz Biotechnology, Inc.), anti-Dnmt1 (sc-20701; Santa Cruz Biotechnology, Inc.), anti-Suz12 (Abcam), and normal rabbit IgG (Santa Cruz Biotechnology, Inc.). An mAb specific for mouse Ring1b was provided by H. Koseki (Riken Research for Allergy and Immunology, Yokohama, Japan). The specific primers used in ChIP assay are shown in Table S1, which is available at http://www.jem.org/cgi/content/full/jem.20072000/DC1.

MeDIP. MeDIP was performed using a METHYL kit (Diagenode). In brief, genomic DNA was purified from effector Th2 cells and sheared by sonication to reduce DNA lengths to between 200 and 1,000 bp. The sheared DNA was diluted and incubated with antiserum specific for the 5-methyl cytidine. Next, immune complexes were precipitated with protein A agarose. The precipitated DNA was purified using QIAquick PCR Purification kit (QIAGEN).

Assessment of memory Th2 cell function in vivo. OVA-specific wild-type and $Bmi1^{-/-}$ effector Th2 cells (10^7 cells) were intravenously transferred into BALB/c *nu/nu* mice. 5 wk after cell transfer, the mice were challenged four times by inhalation with OVA on days 0, 2, 8, and 10. The serum Ig levels, lung histology, mRNA expression in the lung, and airway hyperresponsiveness were then assessed on day 11 as described previously (36, 60). BAL fluid was collected on day 12.

Statistical analysis. Student's *t* test was used.

Online supplemental material. Fig. S1 shows the phenotypic and functional characterization of $Bmi1^{-/-}$ Th2 cells. Fig. S2 shows the impaired generation of memory Th1 cells from $Bmi1^{-/-}$ effector Th1 cells. Fig. S3 depicts the kinetic analysis of the number of Th2 cells after adoptive transfer of effector Th2 cells, and Fig. S4 displays the competitive analysis for memory Th2 cell generation from $Bmi1^{+/+}$ and $Bmi1^{+/-}$ effector Th2 cells under nonlymphopenic conditions. Fig. S5 shows a competitive analysis for memory Th2 cell generation from $Bmi1^{+/+}$ and $Bmi1^{-/-}$ effector Th2 cells under lymphopenic conditions. Fig. S6 shows that deletion of the *p53* gene failed to restore the generation of $Bmi1^{+/-}$ memory Th2 cells. In Fig. S7, mRNA expression of *Noxa* in $Bmi1^{+/+}$ and $Bmi1^{-/-}$ effector Th1, Th2, Tc1, and Tc2 cells is shown. Fig. S8 displays mRNA expression of the *Ink4a/Arf* and *Noxa* in $Bmi1^{+/+}$, $Bmi1^{+/-}$, and $Bmi1^{-/-}$ effector Th2 cells. In Fig. S9, binding of Bmi1 at the Noxa gene locus in effector Th1 and Th2 cells is shown. Fig. S10 depicts histone modifications at the Noxa gene locus in $Bmi1^{+/+}$and $Bmi1^{+/-}$ effector Th1 cells. Fig. S11 shows binding of Dnmt1 at the Noxa gene locus in $Bmi1^{+/+}$and $Bmi1^{+/-}$ effector Th1 cells, and Fig. S12

shows histone modifications at the *Noxa* gene locus after 5-Aza treatment. Fig. S12 displays Noxa mRNA expression and the binding of Bmi1 at the Noxa gene locus in effector Th1 cells after 5-Aza treatment. In Fig. S14, mRNA expression of Noxa in Th2 cells treated with RG108, a DNA methyltransferase inhibitor is shown. Table S1 lists the primer pairs used for the ChIP assay. The online supplemental material is available at http://www.jem.org/cgi/content/full/jem.20072000/DC1.

The authors are grateful to Dr. Ralph T. Kubo for helpful comments and constructive criticism in the preparation of the manuscript. We thank Ms. Hikari Asou, Ms. Satoko Norikane, Ms. Kaoru Sugaya, and Mr. Toshihiro Ito for their excellent technical assistance.

This work was supported by grants from the Ministry of Education, Culture, Sports, Science and Technology (Japan) (Grants-in-Aid: for Scientific Research on Priority Areas no. 17016010; Scientific Research [B] no. 17390139, Scientific Research [C] nos. 18590466, 19590491, and 19591609, Exploratory Research no. 19659121, Young Scientists [Start-up] no. 18890046, and Special Coordination Funds for Promoting Science and Technology), and the Ministry of Health, Labor and Welfare (Japan), Kanae Foundation, Uehara Memorial Foundation, Mochida Foundation, Yasuda Medical Foundation, Astellas Foundation, and Sagawa Foundation.

The authors have no conflicting financial interests.

Submitted: 17 September 2007
Accepted: 26 March 2008

REFERENCES

1. Mosmann, T.R., H. Cherwinski, M.W. Bond, M.A. Giedlin, and R.L. Coffman. 1986. Two types of murine helper T cell clone. I. Definition according to profiles of lymphokine activities and secreted proteins. *J. Immunol.* 136:2348–2357.
2. Seder, R.A., and W.E. Paul. 1994. Acquisition of lymphokine-producing phenotype by CD4$^+$ T cells. *Annu. Rev. Immunol.* 12:635–673.
3. Reiner, S.L., and R.M. Locksley. 1995. The regulation of immunity to Leishmania major. *Annu. Rev. Immunol.* 13:151–177.
4. Kaech, S.M., E.J. Wherry, and R. Ahmed. 2002. Effector and memory T-cell differentiation: implications for vaccine development. *Nat. Rev. Immunol.* 2:251–262.
5. Schluns, K.S., and L. Lefrancois. 2003. Cytokine control of memory T-cell development and survival. *Nat. Rev. Immunol.* 3:269–279.
6. Lanzavecchia, A., and F. Sallusto. 2002. Progressive differentiation and selection of the fittest in the immune response. *Nat. Rev. Immunol.* 2:982–987.
7. Dutton, R.W., L.M. Bradley, and S.L. Swain. 1998. T cell memory. *Annu. Rev. Immunol.* 16:201–223.
8. Sprent, J., and C.D. Surh. 2002. T cell memory. *Annu. Rev. Immunol.* 20:551–579.
9. Lantz, O., I. Grandjean, P. Matzinger, and J.P. Di Santo. 2000. γ chain required for naive CD4$^+$ T cell survival but not for antigen proliferation. *Nat. Immunol.* 1:54–58.
10. Tan, J.T., B. Ernst, W.C. Kieper, E. LeRoy, J. Sprent, and C.D. Surh. 2002. Interleukin (IL)-15 and IL-7 jointly regulate homeostatic proliferation of memory phenotype CD8$^+$ cells but are not required for memory phenotype CD4$^+$ cells. *J. Exp. Med.* 195:1523–1532.
11. Kondrack, R.M., J. Harbertson, J.T. Tan, M.E. McBreen, C.D. Surh, and L.M. Bradley. 2003. Interleukin 7 regulates the survival and generation of memory CD4 cells. *J. Exp. Med.* 198:1797–1806.
12. Li, J., G. Huston, and S.L. Swain. 2003. IL-7 promotes the transition of CD4 effectors to persistent memory cells. *J. Exp. Med.* 198:1807–1815.
13. Seddon, B., P. Tomlinson, and R. Zamoyska. 2003. Interleukin 7 and T cell receptor signals regulate homeostasis of CD4 memory cells. *Nat. Immunol.* 4:680–686.
14. Kaech, S.M., J.T. Tan, E.J. Wherry, B.T. Konieczny, C.D. Surh, and R. Ahmed. 2003. Selective expression of the interleukin 7 receptor identifies effector CD8 T cells that give rise to long-lived memory cells. *Nat. Immunol.* 4:1191–1198.
15. Maraskovsky, E., L.A. O'Reilly, M. Teepe, L.M. Corcoran, J.J. Peschon, and A. Strasser. 1997. Bcl-2 can rescue T lymphocyte development in interleukin-7 receptor-deficient mice but not in mutant rag-1$^{-/-}$ mice. *Cell.* 89:1011–1019.
16. Opferman, J.T., H. Iwasaki, C.C. Ong, H. Suh, S. Mizuno, K. Akashi, and S.J. Korsmeyer. 2005. Obligate role of anti-apoptotic MCL-1 in the survival of hematopoietic stem cells. *Science.* 307:1101–1104.
17. Masopust, D., S.M. Kaech, E.J. Wherry, and R. Ahmed. 2004. The role of programming in memory T-cell development. *Curr. Opin. Immunol.* 16:217–225.
18. Fearon, D.T., P. Manders, and S.D. Wagner. 2001. Arrested differentiation, the self-renewing memory lymphocyte, and vaccination. *Science.* 293:248–250.
19. Luckey, C.J., D. Bhattacharya, A.W. Goldrath, I.L. Weissman, C. Benoist, and D. Mathis. 2006. Memory T and memory B cells share a transcriptional program of self-renewal with long-term hematopoietic stem cells. *Proc. Natl. Acad. Sci. USA.* 103:3304–3309.
20. Park, I.K., D. Qian, M. Kiel, M.W. Becker, M. Pihalja, I.L. Weissman, S.J. Morrison, and M.F. Clarke. 2003. Bmi-1 is required for maintenance of adult self-renewing haematopoietic stem cells. *Nature.* 423:302–305.
21. Iwama, A., H. Oguro, M. Negishi, Y. Kato, Y. Morita, H. Tsukui, H. Ema, T. Kamijo, Y. Katoh-Fukui, H. Koseki, et al. 2004. Enhanced self-renewal of hematopoietic stem cells mediated by the polycomb gene product Bmi-1. *Immunity.* 21:843–851.
22. Molofsky, A.V., R. Pardal, T. Iwashita, I.K. Park, M.F. Clarke, and S.J. Morrison. 2003. *Bmi-1* dependence distinguishes neural stem cell self-renewal from progenitor proliferation. *Nature.* 425:962–967.
23. Lessard, J., and G. Sauvageau. 2003. *Bmi-1* determines the proliferative capacity of normal and leukaemic stem cells. *Nature.* 423:255–260.
24. Satijn, D.P., and A.P. Otte. 1999. Polycomb group protein complexes: do different complexes regulate distinct target genes? *Biochim. Biophys. Acta.* 1447:1–16.
25. van Lohuizen, M. 1999. The trithorax-group and polycomb-group chromatin modifiers: implications for disease. *Curr. Opin. Genet. Dev.* 9:355–361.
26. Cao, R., L. Wang, H. Wang, L. Xia, H. Erdjument-Bromage, P. Tempst, R.S. Jones, and Y. Zhang. 2002. Role of histone H3 lysine 27 methylation in Polycomb-group silencing. *Science.* 298:1039–1043.
27. Kuzmichev, A., K. Nishioka, H. Erdjument-Bromage, P. Tempst, and D. Reinberg. 2002. Histone methyltransferase activity associated with a human multiprotein complex containing the Enhancer of Zeste protein. *Genes Dev.* 16:2893–2905.
28. Czermin, B., R. Melfi, D. McCabe, V. Seitz, A. Imhof, and V. Pirrotta. 2002. *Drosophila* enhancer of Zeste/ESC complexes have a histone H3 methyltransferase activity that marks chromosomal Polycomb sites. *Cell.* 111:185–196.
29. Muller, J., C.M. Hart, N.J. Francis, M.L. Vargas, A. Sengupta, B. Wild, E.L. Miller, M.B. O'Connor, R.E. Kingston, and J.A. Simon. 2002. Histone methyltransferase activity of a *Drosophila* Polycomb group repressor complex. *Cell.* 111:197–208.
30. van der Lugt, N.M., J. Domen, K. Linders, M. van Roon, E. Robanus-Maandag, H. te Riele, M. van der Valk, J. Deschamps, M. Sofroniew, M. van Lohuizen, et al. 1994. Posterior transformation, neurological abnormalities, and severe hematopoietic defects in mice with a targeted deletion of the *bmi-1* proto-oncogene. *Genes Dev.* 8:757–769.
31. Akasaka, T., K. Tsuji, H. Kawahira, M. Kanno, K. Harigaya, L. Hu, Y. Ebihara, T. Nakahata, O. Tetsu, M. Taniguchi, and H. Koseki. 1997. The role of *mel-18*, a mammalian *Polycomb* group gene, during IL-7-dependent proliferation of lymphocyte precursors. *Immunity.* 7:135–146.
32. Kimura, M., Y. Koseki, M. Yamashita, N. Watanabe, C. Shimizu, T. Katsumoto, T. Kitamura, M. Taniguchi, H. Koseki, and T. Nakayama. 2001. Regulation of Th2 cell differentiation by *mel-18*, a mammalian *polycomb* group gene. *Immunity.* 15:275–287.
33. Hosokawa, H., M.Y. Kimura, R. Shinnakasu, A. Suzuki, T. Miki, H. Koseki, M. van Lohuizen, M. Yamashita, and T. Nakayama. 2006. Regulation of Th2 cell development by *Polycomb* group gene *bmi-1* through the stabilization of GATA3. *J. Immunol.* 177:7656–7664.
34. Su, I.H., A. Basavaraj, A.N. Krutchinsky, O. Hobert, A. Ullrich, B.T. Chait, and A. Tarakhovsky. 2003. Ezh2 controls B cell development through histone H3 methylation and *Igh* rearrangement. *Nat. Immunol.* 4:124–131.

35. Yamashita, M., R. Shinnakasu, Y. Nigo, M. Kimura, A. Hasegawa, M. Taniguchi, and T. Nakayama. 2004. Interleukin (IL)-4-independent maintenance of histone modification of the IL-4 gene loci in memory Th2 cells. *J. Biol. Chem.* 279:39454–39464.
36. Yamashita, M., K. Hirahara, R. Shinnakasu, H. Hosokawa, S. Norikane, M.Y. Kimura, A. Hasegawa, and T. Nakayama. 2006. Crucial role of MLL for the maintenance of memory T helper type 2 cell responses. *Immunity.* 24:611–622.
37. Jacobs, J.J., K. Kieboom, S. Marino, R.A. DePinho, and M. van Lohuizen. 1999. The oncogene and Polycomb-group gene *bmi-1* regulates cell proliferation and senescence through the *ink4a* locus. *Nature.* 397:164–168.
38. Lowe, S.W., and C.J. Sherr. 2003. Tumor suppression by *Ink4a-Arf*: progress and puzzles. *Curr. Opin. Genet. Dev.* 13:77–83.
39. Strasser, A. 2005. The role of BH3-only proteins in the immune system. *Nat. Rev. Immunol.* 5:189–200.
40. Alves, N.L., I.A. Derks, E. Berk, R. Spijker, R.A. van Lier, and E. Eldering. 2006. The Noxa/Mcl-1 axis regulates susceptibility to apoptosis under glucose limitation in dividing T cells. *Immunity.* 24:703–716.
41. Marrack, P., and J. Kappler. 2004. Control of T cell viability. *Annu. Rev. Immunol.* 22:765–787.
42. Willis, S.N., and J.M. Adams. 2005. Life in the balance: how BH3-only proteins induce apoptosis. *Curr. Opin. Cell Biol.* 17:617–625.
43. Opferman, J.T., A. Letai, C. Beard, M.D. Sorcinelli, C.C. Ong, and S.J. Korsmeyer. 2003. Development and maintenance of B and T lymphocytes requires antiapoptotic MCL-1. *Nature.* 426:671–676.
44. Oda, E., R. Ohki, H. Murasawa, J. Nemoto, T. Shibue, T. Yamashita, T. Tokino, T. Taniguchi, and N. Tanaka. 2000. Noxa, a BH3-only member of the Bcl-2 family and candidate mediator of p53-induced apoptosis. *Science.* 288:1053–1058.
45. Bruggeman, S.W., M.E. Valk-Lingbeek, P.P. van der Stoop, J.J. Jacobs, K. Kieboom, E. Tanger, D. Hulsman, C. Leung, Y. Arsenijevic, S. Marino, and M. van Lohuizen. 2005. Ink4a and Arf differentially affect cell proliferation and neural stem cell self-renewal in Bmi1-deficient mice. *Genes Dev.* 19:1438–1443.
46. Molofsky, A.V., S. He, M. Bydon, S.J. Morrison, and R. Pardal. 2005. Bmi-1 promotes neural stem cell self-renewal and neural development but not mouse growth and survival by repressing the p16Ink4a and p19Arf senescence pathways. *Genes Dev.* 19:1432–1437.
47. Bauer, A., A. Villunger, V. Labi, S.F. Fischer, A. Strasser, H. Wagner, R.M. Schmid, and G. Hacker. 2006. The NF-κB regulator Bcl-3 and the BH3-only proteins Bim and Puma control the death of activated T cells. *Proc. Natl. Acad. Sci. USA.* 103:10979–10984.
48. You, H., M. Pellegrini, K. Tsuchihara, K. Yamamoto, G. Hacker, M. Erlacher, A. Villunger, and T.W. Mak. 2006. FOXO3a-dependent regulation of Puma in response to cytokine/growth factor withdrawal. *J. Exp. Med.* 203:1657–1663.
49. de Napoles, M., J.E. Mermoud, R. Wakao, Y.A. Tang, M. Endoh, R. Appanah, T.B. Nesterova, J. Silva, A.P. Otte, M. Vidal, et al. 2004. Polycomb group proteins Ring1A/B link ubiquitylation of histone H2A to heritable gene silencing and X inactivation. *Dev. Cell.* 7:663–676.
50. Wang, H., L. Wang, H. Erdjument-Bromage, M. Vidal, P. Tempst, R.S. Jones, and Y. Zhang. 2004. Role of histone H2A ubiquitination in Polycomb silencing. *Nature.* 431:873–878.
51. Cao, R., Y. Tsukada, and Y. Zhang. 2005. Role of Bmi-1 and Ring1A in H2A ubiquitylation and Hox gene silencing. *Mol. Cell.* 20:845–854.
52. Wang, L., J.L. Brown, R. Cao, Y. Zhang, J.A. Kassis, and R.S. Jones. 2004. Hierarchical recruitment of polycomb group silencing complexes. *Mol. Cell.* 14:637–646.
53. Fischle, W., Y. Wang, S.A. Jacobs, Y. Kim, C.D. Allis, and S. Khorasanizadeh. 2003. Molecular basis for the discrimination of repressive methyl-lysine marks in histone H3 by Polycomb and HP1 chromodomains. *Genes Dev.* 17:1870–1881.
54. Min, J., Y. Zhang, and R.M. Xu. 2003. Structural basis for specific binding of Polycomb chromodomain to histone H3 methylated at Lys 27. *Genes Dev.* 17:1823–1828.
55. Vire, E., C. Brenner, R. Deplus, L. Blanchon, M. Fraga, C. Didelot, L. Morey, A. Van Eynde, D. Bernard, J.M. Vanderwinden, et al. 2006. The Polycomb group protein EZH2 directly controls DNA methylation. *Nature.* 439:871–874.
56. Negishi, M., A. Saraya, S. Miyagi, K. Nagao, Y. Inagaki, M. Nishikawa, S. Tajima, H. Koseki, H. Tsuda, Y. Takasaki, et al. 2007. Bmi1 cooperates with Dnmt1-associated protein 1 in gene silencing. *Biochem. Biophys. Res. Commun.* 353:992–998.
57. Murphy, K.M., A.B. Heimberger, and D.Y. Loh. 1990. Induction by antigen of intrathymic apoptosis of $CD4^+CD8^+TCR^{lo}$ thymocytes in vivo. *Science.* 250:1720–1723.
58. Miyoshi, H., U. Blomer, M. Takahashi, F.H. Gage, and I.M. Verma. 1998. Development of a self-inactivating lentivirus vector. *J. Virol.* 72:8150–8157.
59. Yamashita, M., M. Ukai-Tadenuma, M. Kimura, M. Omori, M. Inami, M. Taniguchi, and T. Nakayama. 2002. Identification of a conserved GATA3 response element upstream proximal from the interleukin-13 gene locus. *J. Biol. Chem.* 277:42399–42408.
60. Kamata, T., M. Yamashita, M. Kimura, K. Murata, M. Inami, C. Shimizu, K. Sugaya, C.R. Wang, M. Taniguchi, and T. Nakayama. 2003. *src* homology 2 domain-containing tyrosine phosphatase SHP-1 controls the development of allergic airway inflammation. *J. Clin. Invest.* 111:109–119.

Repressor of GATA regulates T_H2-driven allergic airway inflammation and airway hyperresponsiveness

Kiyoshi Hirahara, MD,[a,b] Masakatsu Yamashita, PhD,[a] Chiaki Iwamura, PhD,[a] Kenta Shinoda, MS,[a] Akihiro Hasegawa, PhD,[a] Hirohisa Yoshizawa, MD,[c] Haruhiko Koseki, MD,[d] Fumitake Gejyo, MD,[b] and Toshinori Nakayama, MD[a] *Chiba, Niigata, and Yokohama, Japan*

Background: Studies of human asthma and of animal models of allergic inflammation/asthma highlight a crucial role for T_H2 cells in the pathogenesis of allergic asthma. Repressor of GATA (ROG) is a POZ (BTB) domain–containing Kruppel-type zinc finger family (or POK family) repressor. A repressive function to GATA3, a master transcription factor for T_H2 cell differentiation, is indicated.

Objective: The aim of this study was to clarify the regulatory roles of ROG in the pathogenesis of T_H2-driven allergic diseases, such as allergic asthma.

Methods: We examined allergic airway inflammation and airway hyperresponsiveness (AHR) in 3 different mouse models, which use either ROG-deficient ($ROG^{-/-}$) mice, ROG transgenic mice, or adoptive transfer of cells.

Results: In $ROG^{-/-}$ mice T_H2 cell differentiation, T_H2 responses, eosinophilic airway inflammation, and AHR were enhanced. In ROG transgenic mice the levels of eosinophilic airway inflammation and AHR were dramatically reduced. Furthermore, adoptive transfer of T_H2 cells with increased or decreased levels of ROG expression into the asthmatic mice resulted in reduced or enhanced airway inflammation, respectively.

Conclusion: These results indicate that ROG regulates allergic airway inflammation and AHR in a negative manner, and thus ROG might represent another potential therapeutic target for the treatment of asthmatic patients. (J Allergy Clin Immunol 2008;122:512-20.)

Key words: Repressor of GATA, POK family, repressor, airway inflammation, airway hyperresponsiveness, GATA3, T_H2, allergic asthma

Abbreviations used
AHR: Airway hyperresponsiveness
APC: Antigen-presenting cell
BAL: Bronchoalveolar lavage
H&E: Hematoxylin and eosin
MDC: Macrophage-derived chemokine
OVA: Ovalbumin
PAS: Periodic acid–Schiff
PLZF: Promyelocytic leukemia zinc finger
ROG: Repressor of GATA
TARC: Thymus and activation-regulated chemokine
TCR: T-cell receptor
Tg: Transgenic

Asthma is a major public health problem that has increased markedly in prevalence in the past 2 decades.[1] Asthma is characterized by a chronic inflammatory disease of the lower airways that causes airway hyperresponsiveness (AHR) to a wide variety of specific and nonspecific stimuli.[2,3] The cardinal features of acute asthma are airway inflammation predominated by eosinophils, hypersecretion of mucus, and AHR. A critical role for T_H2 cells in the pathogenesis of allergic asthma has been demonstrated in the studies of human asthma, as well as in animal models of allergic airway inflammation.[4-10]

It is well established that $CD4^+$ effector T_H cells can be categorized into 3 subsets: T_H1, T_H2, and T_H17 cells. T_H1 cells produce large amounts of IFN-γ and direct cell-mediated immunity against intracellular pathogens. T_H2 cells produce IL-4, IL-5, and IL-13 and are involved in humoral immunity and allergic reactions. Recently, another T_H subset, T_H17, was identified.[11] T_H17 cells produce IL-17 and are involved in the pathogenesis of autoimmune diseases.[12-14] In addition, several transcription factors that control the differentiation of these T_H subsets were identified. Among them, GATA3 appears to be a key transcription factor for T_H2 cell differentiation,[15,16] T-bet for T_H1,[17] and retinoid-related orphan receptor γ t for T_H17 cell differentiation.[18]

GATA3 is selectively induced in developing T_H2 cells after T-cell receptor (TCR) stimulation in the presence of IL-4, and the ectopic expression of GATA3 resulted in the induction of T_H2 cell differentiation in the absence of signal transducer and activator of transcription 6.[19] GATA3 acts as a transcriptional factor for *IL5* and *IL13* genes.[20-22] In addition to the promoter regions, GATA3 also binds to various regulatory regions for T_H2 cytokine expression, including the conserved GATA3 response element,[23] the 3′ site of IL-4,[24] the IL-4/IL-13 intergenic region (conserved noncoding sequence 1),[25] and the 3′ end of the radiation 50 gene.[26] We reported that the histone modifications at the T_H2 cytokine gene loci are primarily mediated through GATA3 in T_H2 and T_C2 (type 2 cytotoxic T) cells.[23,27,28]

From [a]the Department of Immunology, Graduate School of Medicine, Chiba University; [b]the Department of Homeostatic Regulation and Development, Division of Respiratory Medicine, Graduate School of Medical and Dental Sciences, Niigata University; [c]the Bioscience Medical Research Center, Niigata University Medical and Dental Hospital; and [d]the Laboratory for Developmental Biology, RIKEN Research Center for Allergy and Immunology, Yokohama.

Disclosure of potential conflict of interest: The authors have declared that they have no conflict of interest.

Supported by grants from the Ministry of Education, Culture, Sports, Science and Technology (Japan; Grants-in-Aid for Scientific Research on Priority Areas no. 17016010; Scientific Research [B] no. 17390139; Scientific Research [C] nos. 18590466, 19590491, and 19591609; Exploratory Research no. 19659121, and Young Scientists [Start-up] no. 18890046) and Special Coordination Funds for Promoting Science and Technology.

Received for publication February 6, 2008; revised June 2, 2008; accepted for publication June 4, 2008.

Available online July 14, 2008.

Reprint requests: Toshinori Nakayama, MD, Department of Immunology (H3), Graduate School of Medicine, Chiba University, 1-8-1 Inohana, Chuo-ku, Chiba, 260-8670 Japan. E-mail: tnakayama@faculty.chiba-u.jp.

0091-6749/$34.00

doi:10.1016/j.jaci.2008.06.004

The inhibition of GATA3 activity in dominant-negative GATA3 transgenic mice results in a reduction in T_H2 cytokine production and less severe allergic inflammation in a murine model of asthma.[29] Moreover, allergic airway inflammation and AHR have been reported to be compromised by the intranasal administration of antisense GATA3.[30] More recently, in allergen-challenged transgenic mice overexpressing GATA3, airway smooth muscle hyperplasia and subepithelial fibrosis were reported.[31]

Repressor of GATA (ROG) is a POZ (BTB) domain–containing Kruppel-type zinc finger family (or POK family) repressor and is highly homologous to another POK family protein, promyelocytic leukemia zinc finger (PLZF).[32] ROG is also identified as PLZF-like zinc finger protein,[33] testis zinc finger protein,[34] and Fanconi anemia zinc finger.[35] The BTB/POZ domain mediates homodimerization and heterodimerization and recruits corepressor molecules, including histone deacetylases.[36] Two POK family proteins, B-cell lymphoma 6 and PLZF, are known to be implicated in the oncogenic activity in non-Hodgkin's lymphomas[37] and acute promyelocytic leukemia,[38] respectively. Overexpression of ROG exhibited repression of GATA3-induced transactivation of the IL-4 and IL-5 promoters in the M12 B-cell line and the EL-4 T-cell line.[32] We previously reported that the level of ROG is significantly higher in CD8 T cells than in CD4 T cells and that ROG might confer CD8 T cell–specific repression of histone hyperacetylation and activation of the *IL4* gene locus.[27] T cells from ROG-deficient mice showed an increased proliferative response.[33,39] However, the biologic role of ROG in the T_H2 immune responses and the T_H2-dependent diseases has not been investigated.

Here we have established ROG-deficient ($ROG^{-/-}$) mice on either a BALB/c or C57BL/6 background and also ROG-transgenic mice on a C57BL/6 background and used these animals to investigate the role of ROG in T_H1/T_H2 cell differentiation and in the pathogenesis of T_H2-dependent allergic airway inflammation. Our results indicate that ROG negatively regulates T_H2-dependent airway allergic inflammation.

METHODS

Mice

The animals, including $ROG^{-/-}$ mice, used in this study were backcrossed to either BALB/c or C57BL/6 10 times. $ROG^{-/-}$ x DO11.10 transgenic (Tg) mice (anti-ovalbumin [OVA]–specific TCRαβ Tg),[40] $ROG^{-/-}$ x OT-I or OT-II Tg mice (anti-OVA–specific TCRαβ Tg),[41,42] and ROG Tg x OT-I or OT-II Tg mice were used at 6 to 8 weeks of age. BALB/c, C57BL/6, and BALB/c *nu/nu* mice were purchased from Clea, Inc (Tokyo, Japan). All mice used in this study were maintained under specific pathogen-free conditions. Animal care was conducted in accordance with the guidelines of Chiba University.

Immunofluorescent staining and flow cytometric analysis

In general, one million cells were stained with antibodies, as indicated, according to a standard method.[43,44]

Quantitative RT-PCR

Quantitative RT-PCR was performed as described previously with an ABI PRISM 7500 Sequence Detection System (Applied Biosystems, Foster City, Calif) under standard conditions.[45,46] The primers for TaqMan probes for the detection of ROG (exon 2-3), IL-4, IL-5, IL-13, eotaxin 2, RANTES, TNF-α, macrophage-derived chemokine (MDC), thymus and activation-regulated chemokine (TARC), and hypoxanthine-guanine-phosphoribosyl transferase were purchased from Applied Biosystems.

ELISA

Cytokine production was assessed by means of ELISA, as described previously.[44]

In vitro T_H1/T_H2 cell differentiation cultures

A detailed protocol is described in the Methods section available in the Online Repository at www.jacionline.org.

OVA sensitization, inhalation, and analysis of airway inflammation

A detailed protocol is described in the Methods section in the Online Repository.

Statistical analysis

The significance between 2 groups was determined by using the 2-tailed Student *t* test. Comparisons for all pairs were performed with the Kruskal-Wallis test.

RESULTS

Enhanced OVA-induced eosinophilic inflammation and AHR in $ROG^{-/-}$ mice

We generated $ROG^{-/-}$ mice, in which *ROG* mRNA was not expressed in the thymus and peripheral T cells (see Fig E1, *C*, in this article's Online Repository at www.jacionline.org). T-cell development in $ROG^{-/-}$ mice appeared to be normal because no apparent difference in the cellularity and CD4/CD8 ratio in the thymus and spleen compared with that seen in wild-type control animals was observed (see Fig E1, *D*). The cell-surface expression of TCRβ, CD3ε, CD25, CD69, CD44, CD62L, common γ (Cγ), IL-2Rβ, IL-4Rα, and IL-7Rα was normal in $ROG^{-/-}$ splenic CD4 and CD8 T cells (see Fig E1, *E*).

The bronchoalveolar lavage (BAL) fluid of OVA-immunized, OVA-inhaled $ROG^{+/+}$, and $ROG^{-/-}$ mice was collected 48 hours after the last OVA challenge to assess the role of ROG in allergic airway inflammation (see Fig E2 in this article's Online Repository at www.jacionline.org). Significantly increased infiltration of eosinophils and lymphocytes in the antigen-challenged $ROG^{-/-}$ group was detected, whereas the OVA-immunized and PBS-challenged $ROG^{-/-}$ mice did not have airway eosinophilia or show signs of abnormal cellular infiltrates in the BAL fluid (Fig 1, *A*). Evaluation of histologic changes in the lungs of $ROG^{-/-}$ mice by means of hematoxylin and eosin (H&E) staining revealed that the levels of OVA-induced inflammatory mononuclear cell infiltrates in the peribronchiolar region were higher in $ROG^{-/-}$ mice in comparison with the infiltrates in wild-type littermates (Fig 1, *B*, upper panel). No inflammatory cell infiltration was detected in untreated $ROG^{-/-}$ mice (data not shown) or OVA-immunized and PBS-challenged $ROG^{-/-}$ mice. Significant augmentation of eosinophil infiltration was revealed by means of LUNA staining in $ROG^{-/-}$ mice (Fig 1, *B*, lower panel), and as demonstrated by means of periodic acid–Schiff (PAS) staining, enhanced hypermucus production was detected in $ROG^{-/-}$ mice (Fig 1, *C*, and see Fig E3, *A*, in this article's Online Repository at www.jacionline.org). To assess the extent of AHR, we measured the methacholine-induced airflow obstruction

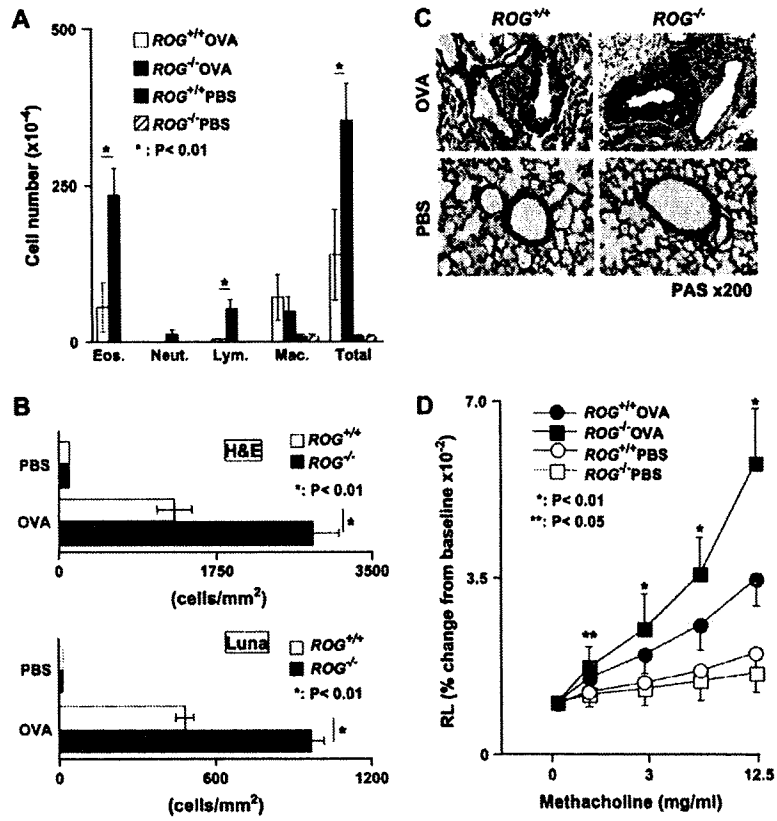

FIG 1. Increased OVA-induced airway inflammation and AHR in $ROG^{-/-}$ mice. **A**, $ROG^{+/+}$ and $ROG^{-/-}$ mice were sensitized with OVA and underwent inhalation with OVA. Infiltrated leukocytes in BAL fluid were assessed. The absolute cell number of eosinophils *(Eos.)*, neutrophils *(Neut.)*, lymphocytes *(Lym.)*, and macrophages *(Mac.)* in the BAL fluid are shown with SDs. Seven to 8 mice per group were used. Three independent experiments were performed, and similar results were obtained. $*P < .01$, Student *t* test. **B**, Semiquantitative analysis of peribronchiolar leukocyte and eosinophil infiltration in the lung. $*P < .01$, Student *t* test. **C**, Hypermucus production was detected in $ROG^{-/-}$ mice. **D**, AHR was assessed as airway resistance *(RL)*. Mean values (5 mice per group) are shown with SDs. $*P < .01$ and $**P < .05$, Kruskal-Wallis test.

in an invasive assay for lung resistance at 24 hours after the last OVA challenge. The mice were anesthetized, tracheostomized, and mechanically ventilated, and lung resistance was measured directly. As expected, lung resistance was also significantly increased in $ROG^{-/-}$ mice in comparison with that seen in $ROG^{+/+}$ mice (Fig 1, *D*). Neither PBS-challenged wild-type nor PBS-challenged $ROG^{-/-}$ mice had AHR. Approximately 2-fold enhancement of AHR was seen at all doses of methacholine in $ROG^{-/-}$ mice in a whole-body plethysmograph (see Fig E3, *B*). Similar enhancement in the levels of eosinophilic inflammation and AHR was observed in $ROG^{-/-}$ mice with a C57BL/6 background (data not shown). These results indicate that the extent of OVA-induced airway inflammation and AHR is enhanced in $ROG^{-/-}$ mice.

Enhanced OVA-induced T_H2 immune response in $ROG^{-/-}$ mice

Proliferative responses induced by anti-TCR mAb stimulation (see Fig E4, *A*, in this article's Online Repository at www.jaci online.org) or antigenic peptide stimulation (see Fig E4, *C*) were significantly higher in $ROG^{-/-}$ CD4 and CD8 T cells. The rate of cell division after antigen stimulation was also moderately higher in $ROG^{-/-}$ mice (see Fig E4, *B*). An assessment of the capability of $ROG^{-/-}$ CD4 T cells to differentiate into T_H1/T_H2 cells *in vitro* indicated moderate enhancement in T_H2 cell differentiation under T_H2 conditions (34.9% vs 44.9% and 27.8% vs 37.6%; Fig 2, *A*) and under neutral conditions (3.0% vs 8.7% and 15.3% vs 26.7%; see Fig E5 in this article's Online Repository at www.jacionline.org), whereas T_H1 cell differentiation was equivalent (Fig 2, *A*).

We then examined the expression levels of IL-4, IL-5, IL-13, eotaxin 2, RANTES, and TNF-α in the BAL fluid cells of OVA-sensitized and OVA-challenged $ROG^{-/-}$ mice shown in Fig 1. Quantitative RT-PCR analysis was performed with RNA isolated from the infiltrates in the BAL fluid. The expression levels of IL-4, IL-5, IL-13, eotaxin 2, and RANTES were higher in $ROG^{-/-}$ mice than in $ROG^{+/+}$ mice, whereas the TNF-α level was comparable (Fig 2, *B*). Moreover, cytokine levels in the BAL fluid, as measured by means of ELISA, showed increased production of IL-5 and IL-13 in $ROG^{-/-}$ BAL fluid (Fig 2, *C*). At the same time, mediastinal lymph nodes were harvested and stained for intracellular IFN-γ and IL-4. Modest but reproducibly increased numbers of IL-4–producing cells were

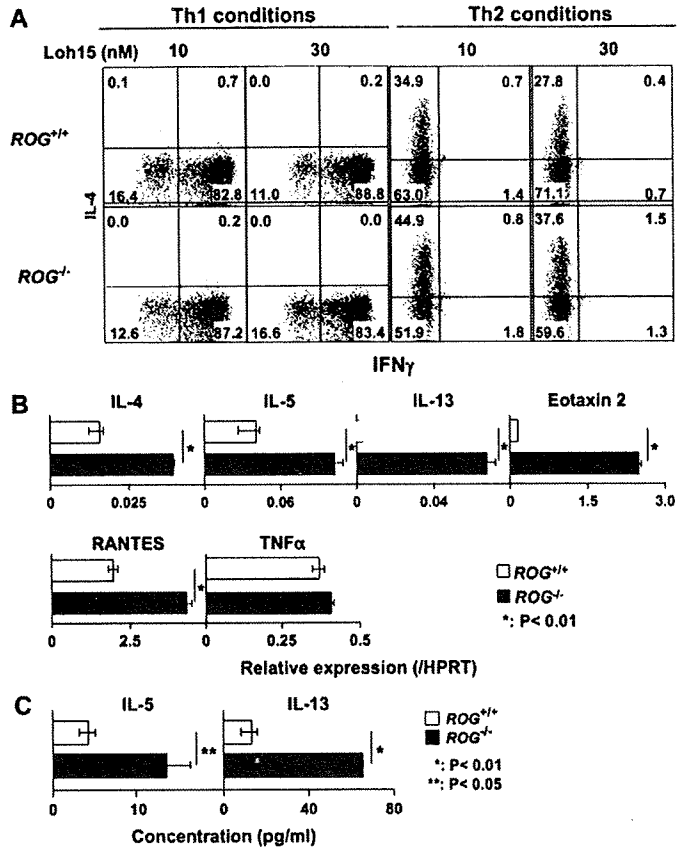

FIG 2. Increased T_H2 cytokine production in the airways of $ROG^{-/-}$ mice. **A**, The ability to differentiate into T_H1/T_H2 cells from $ROG^{-/-}$ x DO11.10 Tg mice was assessed. The results are representative of 5 experiments. **B**, mRNA levels of IL-4, IL-5, IL-13, eotaxin 2, RANTES, and TNF-α in BAL fluid cells were determined by using quantitative RT-PCR. $*P < .01$, Student *t* test. **C**, The amount of IL-5 and IL-13 in the BAL fluid was determined by means of ELISA. The mean values with SDs (3-5 mice per group) are shown. $*P < .01$ and $**P < .05$, Student *t* test.

observed (see Fig E6 in this article's Online Repository at www.jacionline.org). We measured the mRNA expression levels of TARC and MDC, which are known to be the chemokines for T_H cell recruitment by using mRNA from the allergic lung, and no significant difference was noted between $ROG^{+/+}$ and $ROG^{-/-}$ mice (data not shown). Thus the enhanced OVA-induced airway inflammation and AHR observed in $ROG^{-/-}$ mice could be due to the enhanced T_H2 responses in the airways of $ROG^{-/-}$ mice.

Attenuated OVA-induced eosinophilic inflammation and airway AHR in ROG Tg mice

To further investigate the regulatory role of ROG in T cells, we generated ROG Tg mice under the control of a T-cell specific lck proximal promoter (see Fig E7, *A* and *B*, in this article's Online Repository at www.jacionline.org). Quantitative RT-PCR analysis revealed that *ROG* mRNA was expressed 10-fold higher in thymocytes and splenic CD4 and CD8 T cells in ROG Tg mice (see Fig E7, *C*). The cellularity and CD4/CD8 ratio in the thymus and spleen in ROG Tg mice did not differ from those in wild-type mice (see Fig E7, *D*). The cell-surface expression of TCRβ, CD3ε, CD25, CD69, CD44, CD62L, Cγ, IL-2Rβ, IL-4Rα, and IL-7Rα on the splenic CD4 and CD8 T cells from ROG Tg mice was normal (see Fig E7, *E*).

BAL fluid of OVA-immunized and OVA-inhaled wild-type and ROG Tg mice was analyzed to evaluate the extent of T_H2-dependent airway inflammation in ROG Tg mice. The number of total infiltrated cells, lymphocytes, and eosinophils was found to be reduced in ROG Tg mice: the most striking difference between wild-type and ROG Tg mice was the difference in the number of eosinophils (Fig 3, *A*). Histologic examination revealed very low-level infiltrates in the peribronchiolar regions in the lungs of ROG Tg mice (Fig 3, *B*, upper panel). The decreased eosinophilic infiltration in ROG Tg mice was confirmed by means of LUNA staining (Fig 3, *B*, lower panel). Goblet cell metaplasia and mucus hyperproduction were also reduced in ROG Tg mice (Fig 3, *C*, and see Fig E8, *A*, in this article's Online Repository at www.jacionline.org). Lung resistance, as measured by using a direct invasive method, showed no increase in the AHR in ROG Tg mice compared with the increase in wild-type mice (Fig 3, *D*). ROG Tg mice did not have significant AHR, and the sensitivity to methacholine was almost equivalent to that seen in PBS-challenged control mice (see Fig E8, *B*). From these results, we conclude that overexpression of ROG in T cells results in the inhibition of OVA-induced airway inflammation and AHR.

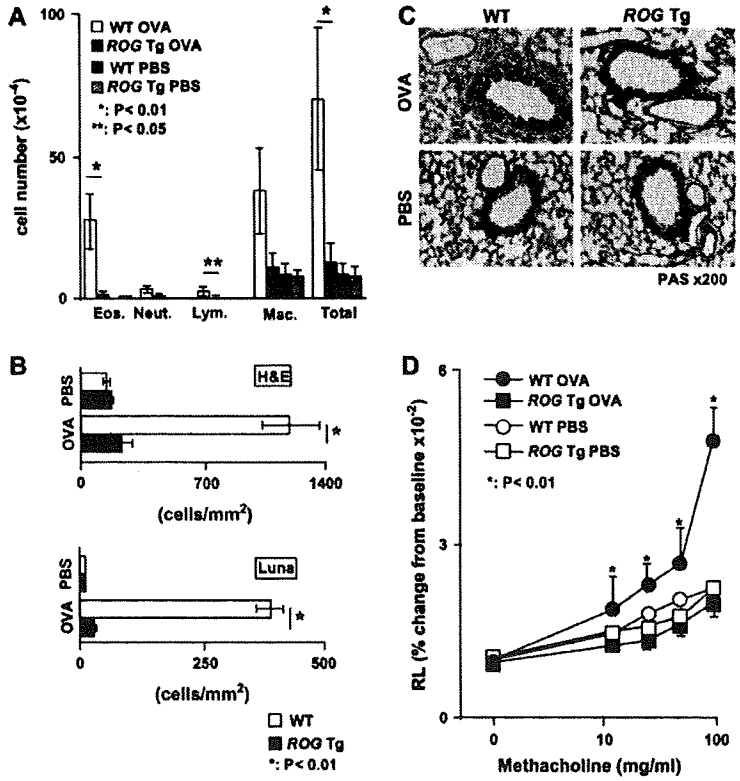

FIG 3. Inhibition of OVA-induced airway inflammation and AHR in ROG Tg mice. **A**, Decreased infiltration of eosinophils in BAL fluid in asthmatic ROG Tg mice. Five mice per group were used. Two independent experiments were performed, and similar results were obtained. $*P < .01$ and $**P < .05$, Student *t* test. **B**, Semiquantitative analysis of peribronchiolar leukocyte infiltrates from H&E-stained *(upper panel)* and LUNA-stained *(lower panel)* samples. $*P < .01$, Student *t* test. **C**, Reduced mucus production in ROG Tg mice sensitized and challenged with OVA. **D**, AHR was assessed in an invasive assay system. Mean values (6 mice per group) are shown with SDs. $*P < .01$, Kruskal-Wallis test. *WT*, Wild-type.

Attenuated T_H2 responses induced by ROG Tg CD4 T cells

Assessment of T_H1/T_H2 cell differentiation of ROG Tg mice showed reduced T_H2 cell differentiation in CD4 T cells from ROG Tg mice compared with that seen in wild-type mice (39.3% vs 27.0% and 30.2% vs 14.8%), whereas T_H1 cell (80.2% vs 77.8% and 64.6% vs 64.4%) differentiation was equivalent (Fig 4, *A*). As expected, proliferative responses of both CD4 and CD8 T cells were reduced in ROG Tg mice (see Fig E9, *A* and *B*, in this article's Online Repository at www.jacionline.org). Consequently, we examined the expression levels of IL-4, IL-5, IL-13, eotaxin 2, RANTES, and TNF-α in the BAL fluid cells of the OVA-sensitized and OVA-challenged ROG Tg mice shown in Fig 3. The expression levels of mRNA for IL-4, IL-5, IL-13, eotaxin 2, and RANTES in Tg mice were clearly lower than those in wild-type mice (Fig 4, *B*). Reduced production of IL-5 and IL-13 in BAL fluids from ROG Tg mice was also confirmed by means of ELISA (Fig 4, *C*). We measured the mRNA expression levels of TARC and MDC using allergic lung samples, and no significant decrease was noted in ROG Tg mice (data not shown). These results indicate that the extent of T_H2 cell differentiation was reduced in ROG Tg CD4 T cells and that T_H2-dependent immune responses in the airway in an allergic asthma model were attenuated.

Decreased airway inflammation in mice after adoptive transfer of ROG-overexpressing T cells

Next we examined whether the retrovirus-mediated overexpression of ROG into effector T_H2 cells would affect downregulation of T_H2 cell–mediated inflammatory responses. As shown in Fig 5, *A*, a modest decrease in the numbers of IL-4–producing T_H2 cells was detected in the retrovirus-mediated ROG-overexpressing cell cultures. One million IL-4–producing cells from each culture were transferred into BALB/c *nu/nu* mice. At 48 and 96 hours after cell transfer, mice were challenged with OVA, and infiltration of inflammatory cells was determined. As shown in Fig 5, *B*, the induction of airway infiltration of leukocytes, including eosinophils, was essentially not observed in the mice adoptively transferred with ROG-introduced T_H2 cells compared with the mice with wild-type T_H2 cells. Consequently, RNA was isolated and quantitative RT-PCR analysis was performed to assess the expression of T_H2 cytokines and chemokines in the infiltrates in BAL fluid. The expression levels of IL-4, IL-5, IL-13, and eotaxin 2 in the mice receiving ROG-introduced cells were lower than those in mice receiving mock-introduced cells, whereas RANTES and TNF-α levels were comparable (Fig 5, *C*). Lung resistance, as measured by using a direct invasive method, showed no obvious increase in the AHR in mice transferred with ROG-introduced cells compared with those with

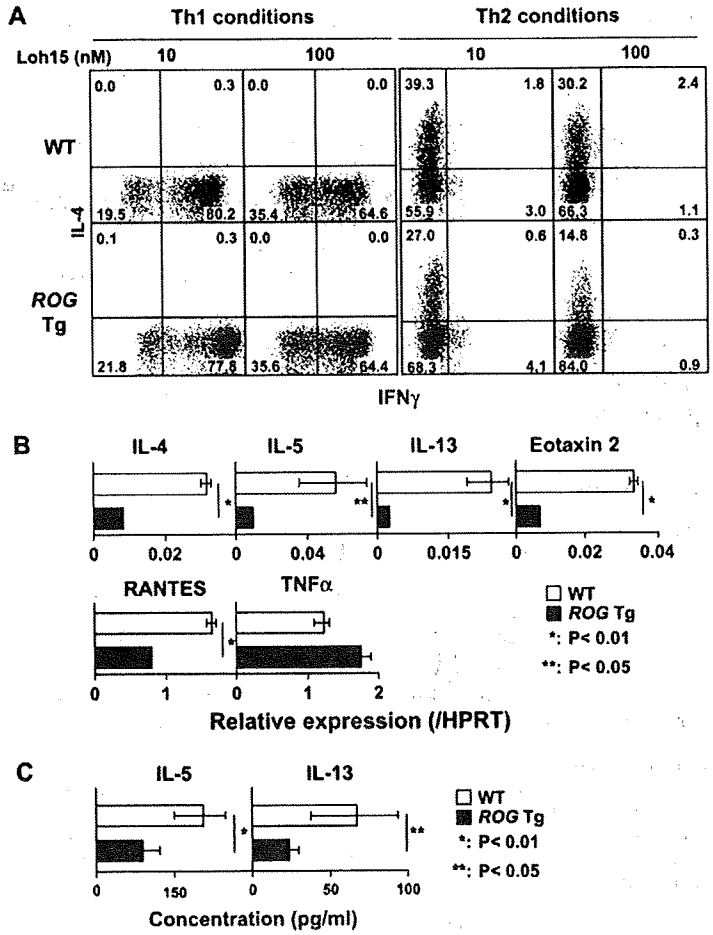

FIG 4. Decreased T_H2 cell differentiation and T_H2 cytokine production in the airways of ROG Tg mice. **A**, The ability to differentiate into T_H1/T_H2 cells *in vitro* in ROG Tg x OT-II transgenic mice was assessed. The results are representative of 5 experiments. **B**, mRNA levels of IL-4, IL-5, IL-13, eotaxin 2, RANTES, and TNF-α in BAL fluid cells of wild-type and ROG Tg mice were determined by means of quantitative RT-PCR. $*P < .01$ and $**P < .05$, Student *t* test. **C**, The amount of IL-5 and IL-13 in the BAL fluid was determined by means of ELISA. The mean values with SDs (4 mice per group) are shown. $*P < .01$ and $**P < .05$, Student *t* test. *WT*, Wild-type.

mock-introduced cells (Fig 5, *D*). These results indicate that the expression levels of ROG in T_H2 cells can affect the OVA-induced airway inflammation.

Modulation of airway inflammation by adoptively transferred *ROG*$^{-/-}$ and ROG Tg T cells

Finally, we addressed whether OVA-primed T cells with altered ROG expression are able to modulate OVA-induced allergic inflammation. After immunization with OVA, splenic CD3 T cells from ROG Tg mice or *ROG*$^{-/-}$ mice (C57BL/6 background) were prepared and transferred into C57BL/6 mice that had been also immunized with OVA twice. Two and 4 days after cell transfer, mice were treated with OVA by means of inhalation, and the inflammatory infiltrates in the BAL fluid were analyzed. As shown in Fig 6, *A*, the adoptive transfer of CD3 T cells from ROG Tg mice significantly reduced the levels of infiltration of leukocytes, especially eosinophils. In contrast, the adoptive transfer of CD3 T cells from *ROG*$^{-/-}$ mice resulted in increased levels of eosinophilic infiltrates. When primed CD3 T cells from ROG Tg mice were used, moderate but significantly decreased numbers of inflammatory mononuclear cells and eosinophils were observed by means of histologic analyses with H&E and LUNA staining (Fig 6, *B*), respectively. A significantly decreased number of PAS-stained cells in the mice receiving ROG Tg T cells was seen, whereas an increased number of these cells was noted in mice receiving *ROG*$^{-/-}$ T-cell transfer (Fig 6, *B*, right panel).

DISCUSSION

Murine models of allergic asthma have been used to dissect the underlying pathogenesis of human asthma. In this study we demonstrate an important role for ROG in the regulation of T_H2-dependent allergen-induced airway inflammation and AHR by using newly established *ROG*$^{-/-}$ and ROG Tg mice with a BALB/c or C57BL/6 background and with a retrovirus-mediated ROG gene-introduction system. T_H2-dependent airway inflammation was enhanced in *ROG*$^{-/-}$ mice (Fig 1) and was dramatically inhibited in ROG Tg mice (Fig 3). We observed moderate enhancement in T_H2 cell differentiation in *ROG*$^{-/-}$ mice, with a marginal effect in T_H1 cell differentiation (Fig 2). In ROG Tg

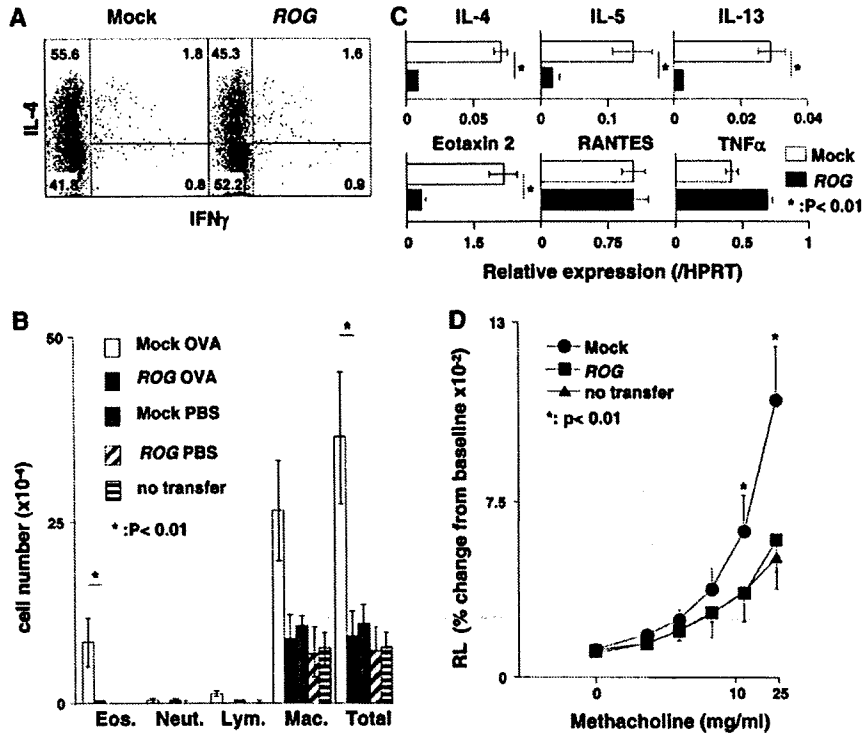

FIG 5. Decreased airway inflammation in mice after adoptive transfer of ROG-overexpressing T cells. A, IFN-γ/IL-4 profiles of the transferred *in vitro* generated T_H2 cells. B, Decreased infiltration of eosinophils in BAL fluid in mice receiving ROG-overexpressing T cells. Five mice per group were used. Two independent experiments were performed, and similar results were obtained. $*P < .01$, Student *t* test. C, mRNA levels of IL-4, IL-5, IL-13, eotaxin 2, RANTES, and TNF-α in the BAL fluid cells from adoptive transfer mice were determined by using quantitative RT-PCR. $*P < .01$, Student *t* test. D, One day after the last OVA inhalation, AHR was assessed, and results are presented as airway resistance *(RL)*. Mean values (5-6 mice per group) are shown with SDs. $*P < .01$, Kruskal-Wallis test.

mice T_H2 cell differentiation was affected, whereas T_H1 cell differentiation was normal (Fig 4). Moreover, retrovirus-mediated ROG-overexpressing T_H2 cells also did not induce airway inflammation in an adoptive transfer model (Fig 5). From these results, we conclude that ROG in T cells plays an important regulatory role in T_H2-dependent inflammatory responses in the airway.

The preferential effect in T_H2 cells might be consistent with the notion that ROG negatively regulates GATA3,[32] which is highly expressed in T_H2 cells.[15,16] ROG regulates in a negative fashion the proliferative responses of CD4 and CD8 T cells after TCR stimulation with $ROG^{-/-}$ and ROG Tg mice (see Figs E4 and E9). Furthermore, the rate of cell division of CD4 and CD8 T cells was moderately higher in $ROG^{-/-}$ mice (see Fig E4, *B*). The levels of enhancement were quite comparable in the previously reported $ROG^{-/-}$ mice.[33,39] Taken together, ROG can exert control of at least 2 different processes in T cells during the induction of T_H2 responses and inflammation: (1) a general process, proliferation of T cells after TCR stimulation, and (2) a T_H2-specific process, the extent of differentiation into T_H2 cells through the regulation of GATA3. In the first process the involvement of the regulation of nuclear factor of activated T cells, cytoplasmic 2 (nuclear factor of activated T cells 1)–initiated suppression of the nuclear factor κB pathway is suggested.[32]

We observed greater effects in cytokine expression and eosinophil numbers in the BAL fluid than in those of IL-4–producing T_H2 cells in *in vitro* intracellular cytokine staining experiments (Figs 1-5). This could be due to the involvement of ROG-mediated regulation of the expansion of T cells *in vivo* in the case of the BAL fluid results. The expression of ROG controls antigen-induced proliferative responses of T cells (see Figs E4 and E9), and therefore the expansion of OVA-specific T cells after OVA inhalation might account for the results seen with the BAL fluid samples (cytokine expression and eosinophil number). In contrast, no T-cell expansion would be expected to occur after restimulation with anti-TCR mAb for 6 hours in the presence of monensin *in vitro*.

In a previous study by Kang et al,[39] no significant changes in the generation of IL-4–producing cells was observed in their $ROG^{-/-}$ mice. However, Piazza et al[33] used an independent line of $ROG^{-/-}$ mice and showed an increased T_H2 cytokine mRNA expression in T_H2 cells, which is consistent with our results. Piazza et al[33] showed a normal expression of the mixed lineage leukemia 2 (*MLL2*), a neighboring gene of ROG, in $ROG^{-/-}$ mice. Normal expression of *MLL2* was confirmed in our $ROG^{-/-}$ mice (data not shown). Kang et al[39] demonstrate that the deficiency of ROG resulted in a marginal effect on the severity of experimental autoimmune encephalomyelitis, a T_H cell–mediated disease. We used a T_H2-dependent experimental asthma model in which we observed a substantial effect. Thus some apparent differences in the results obtained in these studies could be due to the difference in the experimental model systems used. In any event, with our newly established $ROG^{-/-}$ mice and ROG Tg mice, which have been extensively

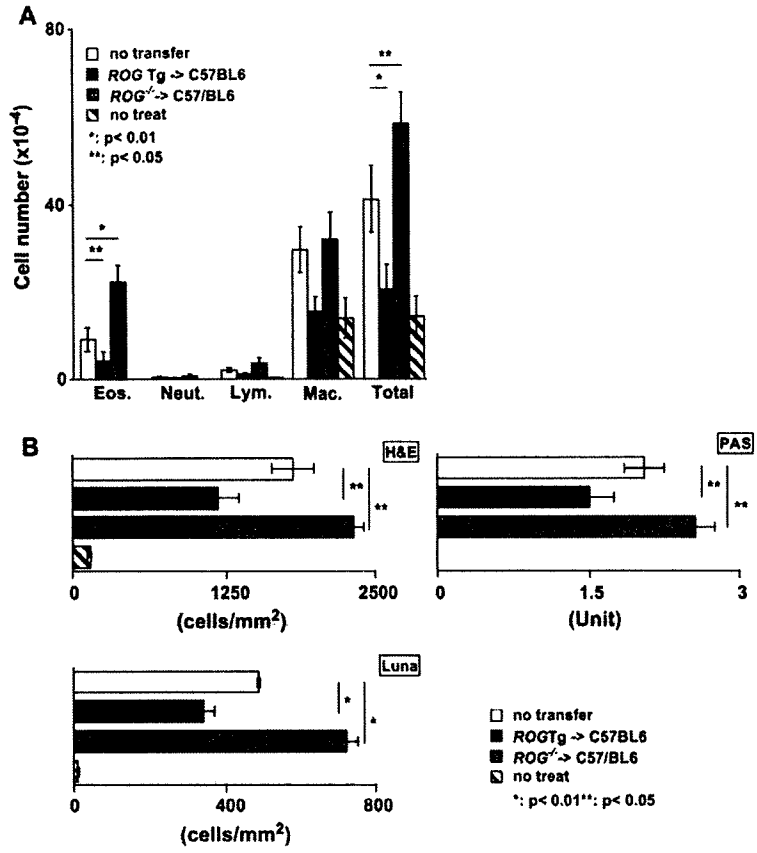

FIG 6. Modulation of airway inflammation by adoptive transfer of *ROG*$^{-/-}$ and ROG Tg T cells. **A**, Donor mice (*ROG*$^{-/-}$ and ROG Tg mice on a C57Bl/6 background) and recipient mice (C57BL/6) were sensitized with OVA. Splenic CD3 T cells were prepared from donor mice and transferred into recipient mice. Infiltrated leukocytes in BAL fluid are shown. Five mice per group were used. $*P < .01$ and $**P < .05$ between groups, Student *t* test. **B**, Semiquantitative analysis of peribronchiolar leukocyte infiltration (H&E stain), peribronchiolar eosinophil infiltration (LUNA stain), and the abundance of PAS-positive mucus containing cells (PAS stain). $*P < .01$ and $**P < .05$ between groups, Student *t* test.

backcrossed on either C57BL/6 or BALB/c backgrounds, we demonstrate clearly that ROG regulates T_H2 cell differentiation and T_H2-dependent inflammation in the airway.

T_H2-dependent airway inflammation was not significantly induced in nude mice after adoptive transfer of effector T_H2 cells expressing increased levels of ROG (Fig 5). In addition, the transfer of ROG Tg T_H2 cells into normal mice that were OVA sensitized and challenged resulted in the inhibition of the T_H2-dependent airway inflammation (Fig 6). This might raise the possibility of the therapeutic potential of the ROG-overexpressing T cells. Adoptive transfer of ROG Tg T cells can compete with antigen-presenting dendritic cells in the airway with the host T_H2 cells that induce T_H2-dependent airway inflammation. Indeed, our preliminary results indicate that ROG Tg CD4 T cells compete efficiently with wild-type CD4 T cells to reduce the wild-type CD4 T-cell proliferation induced by OVA peptide pulsed on dendritic cells (unpublished observation). It was recently reported that during clonal expansion antigen-specific T cells could compete for the limited number of peptide/MHC complex sites on dendritic cells if the number of T cells is abundant.[47]

In summary, our study highlights a role for ROG in the development of eosinophilic inflammation and AHR and suggests that ROG could consequently be another possible therapeutic target for the treatment of allergic asthma.

We thank Drs Ralph T. Kubo and Tsuneyasu Kaisho for helpful comments and constructive criticisms in the preparation of the manuscript.

Key messages

- ROG regulates the pathogenesis of T_H2-driven allergic airway inflammation and AHR.
- ROG might be a potential therapeutic target for the treatment of asthmatic patients.

REFERENCES

1. Eder W, Ege MJ, von Mutius E. The asthma epidemic. N Engl J Med 2006;355:2226-35.
2. McFadden ER Jr, Gilbert IA. Asthma. N Engl J Med 1992;327:1928-37.
3. Busse WW, Lemanske RF Jr. Asthma. N Engl J Med 2001;344:350-62.
4. Hamelmann E, Gelfand EW. IL-5-induced airway eosinophilia—the key to asthma? Immunol Rev 2001;179:182-91.
5. Lloyd CM, Gonzalo JA, Coyle AJ, Gutierrez-Ramos JC. Mouse models of allergic airway disease. Adv Immunol 2001;77:263-95.

6. Elias JA, Lee CG, Zheng T, Ma B, Homer RJ, Zhu Z. New insights into the pathogenesis of asthma. J Clin Invest 2003;111:291-7.
7. Kamata T, Yamashita M, Kimura M, Murata K, Inami M, Shimizu C, et al. src homology 2 domain-containing tyrosine phosphatase SHP-1 controls the development of allergic airway inflammation. J Clin Invest 2003;111:109-19.
8. Wills-Karp M. Interleukin-13 in asthma pathogenesis. Immunol Rev 2004;202: 175-90.
9. Cohn L, Elias JA, Chupp GL. Asthma: mechanisms of disease persistence and progression. Annu Rev Immunol 2004;22:789-815.
10. Umetsu DT, DeKruyff RH. The regulation of allergy and asthma. Immunol Rev 2006;212:238-55.
11. Infante-Duarte C, Horton HF, Byrne MC, Kamradt T. Microbial lipopeptides induce the production of IL-17 in Th cells. J Immunol 2000;165:6107-15.
12. Harrington LE, Hatton RD, Mangan PR, Turner H, Murphy TL, Murphy KM, et al. Interleukin 17-producing CD4+ effector T cells develop via a lineage distinct from the T helper type 1 and 2 lineages. Nat Immunol 2005;6:1123-32.
13. Park H, Li Z, Yang XO, Chang SH, Nurieva R, Wang YH, et al. A distinct lineage of CD4 T cells regulates tissue inflammation by producing interleukin 17. Nat Immunol 2005;6:1133-41.
14. Bettelli E, Oukka M, Kuchroo VK. TH-17 cells in the circle of immunity and autoimmunity. Nat Immunol 2007;8:345-50.
15. Zhang DH, Cohn L, Ray P, Bottomly K, Ray A. Transcription factor GATA-3 is differentially expressed in murine Th1 and Th2 cells and controls Th2-specific expression of the interleukin-5 gene. J Biol Chem 1997;272:21597-603.
16. Zheng W, Flavell RA. The transcription factor GATA-3 is necessary and sufficient for Th2 cytokine gene expression in CD4 T cells. Cell 1997;89:587-96.
17. Szabo SJ, Sullivan BM, Stemmann C, Satoskar AR, Sleckman BP, Glimcher LH. Distinct effects of T-bet in TH1 lineage commitment and IFN-γ production in CD4 and CD8 T cells. Science 2002;295:338-42.
18. Ivanov II, McKenzie BS, Zhou L, Tadokoro CE, Lepelley A, Lafaille JJ, et al. The orphan nuclear receptor RORγt directs the differentiation program of proinflammatory IL-17$^+$ T helper cells. Cell 2006;126:1121-33.
19. Kurata H, Lee HJ, O'Garra A, Arai N. Ectopic expression of activated Stat6 induces the expression of Th2-specific cytokines and transcription factors in developing Th1 cells. Immunity 1999;11:677-88.
20. Lee HJ, O'Garra A, Arai K, Arai N. Characterization of cis-regulatory elements and nuclear factors conferring Th2-specific expression of the IL-5 gene: a role for a GATA-binding protein. J Immunol 1998;160:2343-52.
21. Zhang DH, Yang L, Ray A. Differential responsiveness of the IL-5 and IL-4 genes to transcription factor GATA-3. J Immunol 1998;161:3817-21.
22. Schwenger GT, Fournier R, Kok CC, Mordvinov VA, Yeoman D, Sanderson CJ. GATA-3 has dual regulatory functions in human interleukin-5 transcription. J Biol Chem 2001;276:48502-9.
23. Yamashita M, Ukai-Tadenuma M, Kimura M, Omori M, Inami M, Taniguchi M, et al. Identification of a conserved GATA3 response element upstream proximal from the interleukin-13 gene locus. J Biol Chem 2002;277:42399-408.
24. Agarwal S, Avni O, Rao A. Cell-type-restricted binding of the transcription factor NFAT to a distal IL-4 enhancer in vivo. Immunity 2000;12:643-52.
25. Takemoto N, Kamogawa Y, Jun Lee H, Kurata H, Arai KI, O'Garra A, et al. Cutting edge: chromatin remodeling at the IL-4/IL-13 intergenic regulatory region for Th2-specific cytokine gene cluster. J Immunol 2000;165:6687-91.
26. Fields PE, Lee GR, Kim ST, Bartsevich VV, Flavell RA. Th2-specific chromatin remodeling and enhancer activity in the Th2 cytokine locus control region. Immunity 2004;21:865-76.
27. Omori M, Yamashita M, Inami M, Ukai-Tadenuma M, Kimura M, Nigo Y, et al. CD8 T cell-specific downregulation of histone hyperacetylation and gene activation of the IL-4 gene locus by ROG, repressor of GATA. Immunity 2003;19: 281-94.
28. Inami M, Yamashita M, Tenda Y, Hasegawa A, Kimura M, Hashimoto K, et al. CD28 costimulation controls histone hyperacetylation of the interleukin 5 gene locus in developing Th2 cells. J Biol Chem 2004;279:23123-33.
29. Zhang DH, Yang L, Cohn L, Parkyn L, Homer R, Ray P, et al. Inhibition of allergic inflammation in a murine model of asthma by expression of a dominant-negative mutant of GATA-3. Immunity 1999;11:473-82.
30. Finotto S, De Sanctis GT, Lehr HA, Herz U, Buerke M, Schipp M, et al. Treatment of allergic airway inflammation and hyperresponsiveness by antisense-induced local blockade of GATA-3 expression. J Exp Med 2001;193:1247-60.
31. Kiwamoto T, Ishii Y, Morishima Y, Yoh K, Maeda A, Ishizaki K, et al. Transcription factors T-bet and GATA-3 regulate development of airway remodeling. Am J Respir Crit Care Med 2006;174:142-51.
32. Miaw SC, Choi A, Yu E, Kishikawa H, Ho IC. ROG, repressor of GATA, regulates the expression of cytokine genes. Immunity 2000;12:323-33.
33. Piazza F, Costoya JA, Merghoub T, Hobbs RM, Pandolfi PP. Disruption of PLZP in mice leads to increased T-lymphocyte proliferation, cytokine production, and altered hematopoietic stem cell homeostasis. Mol Cell Biol 2004;24:10456-69.
34. Lin W, Lai CH, Tang CJ, Huang CJ, Tang TK. Identification and gene structure of a novel human PLZF-related transcription factor gene, TZFP. Biochem Biophys Res Commun 1999;264:789-95.
35. Hoatlin ME, Zhi Y, Ball H, Silvey K, Melnick A, Stone S, et al. A novel BTB/POZ transcriptional repressor protein interacts with the Fanconi anemia group C protein and PLZF. Blood 1999;94:3737-47.
36. Bardwell VJ, Treisman R. The POZ domain: a conserved protein-protein interaction motif. Genes Dev 1994;8:1664-77.
37. Lo Coco F, Ye BH, Lista F, Corradini P, Offit K, Knowles DM, et al. Rearrangements of the BCL6 gene in diffuse large cell non-Hodgkin's lymphoma. Blood 1994;83:1757-9.
38. Dong S, Zhu J, Reid A, Strutt P, Guidez F, Zhong HJ, et al. Amino-terminal protein-protein interaction motif (POZ-domain) is responsible for activities of the promyelocytic leukemia zinc finger-retinoic acid receptor-α fusion protein. Proc Natl Acad Sci U S A 1996;93:3624-9.
39. Kang BY, Miaw SC, Ho IC. ROG negatively regulates T-cell activation but is dispensable for Th-cell differentiation. Mol Cell Biol 2005;25:554-62.
40. Murphy KM, Heimberger AB, Loh DY. Induction by antigen of intrathymic apoptosis of CD4+CD8+TCRlo thymocytes in vivo. Science 1990;250:1720-3.
41. Hogquist KA, Jameson SC, Heath WR, Howard JL, Bevan MJ, Carbone FR. T cell receptor antagonist peptides induce positive selection. Cell 1994;76:17-27.
42. Barnden MJ, Allison J, Heath WR, Carbone FR. Defective TCR expression in transgenic mice constructed using cDNA-based α- and β-chain genes under the control of heterologous regulatory elements. Immunol Cell Biol 1998;76:34-40.
43. Nakayama T, June CH, Munitz TI, Sheard M, McCarthy SA, Sharrow SO, et al. Inhibition of T cell receptor expression and function in immature CD4+CD8+ cells by CD4. Science 1990;249:1558-61.
44. Yamashita M, Kimura M, Kubo M, Shimizu C, Tada T, Perlmutter RM, et al. T cell antigen receptor-mediated activation of the Ras/mitogen-activated protein kinase pathway controls interleukin 4 receptor function and type-2 helper T cell differentiation. Proc Natl Acad Sci U S A 1999;96:1024-9.
45. Kimura MY, Hosokawa H, Yamashita M, Hasegawa A, Iwamura C, Watarai H, et al. Regulation of T helper type 2 cell differentiation by murine Schnurri-2. J Exp Med 2005;201:397-408.
46. Nigo YI, Yamashita M, Hirahara K, Shinnakasu R, Inami M, Kimura M, et al. Regulation of allergic airway inflammation through Toll-like receptor 4-mediated modification of mast cell function. Proc Natl Acad Sci U S A 2006;103: 2286-91.
47. Garcia Z, Pradelli E, Celli S, Beuneu H, Simon A, Bousso P. Competition for antigen determines the stability of T cell-dendritic cell interactions during clonal expansion. Proc Natl Acad Sci U S A 2007;104:4553-8.

METHODS

Mice

OT-I Tg mice are OVA-specific, MHC class I–restricted TCRαβ transgenic mice with a C57BL/6 background.[E1] The TCR recognizes a specific OVA peptide (SIIN, OVA 257-264).

OT-II Tg mice are OVA-specific, MHC class II–restricted TCRαβ transgenic mice with a C57BL/6 background.[E2] The TCR recognizes a specific OVA peptide (Loh 15, OVA 323-339). DO11.10 Tg mice are OVA-specific, MHC class II–restricted TCRαβ transgenic mice with a BALB/c background.[E3] The TCR recognizes a specific OVA peptide (Loh 15, OVA 323-339). BALB/c *nu/nu* mice lack the thymus, and no functional T cells are present.

Genetic background of mice used in the study

It has been recognized that BALB/c mice show more prominent T_H2 responses than C57BL/6 mice. To investigate the T_H2-dependent responses *in vivo*, we used $ROG^{-/-}$ mice with a BALB/c background (Figs 1 and 2). We have obtained similar results in $ROG^{-/-}$ mice with a C57BL/6 background (data not shown). We have ROG Tg mice only with a C57BL/6 background, and therefore we used C57BL/6 background mice in the experiments using ROG Tg mice (Figs 3 and 4) and with adoptive transfer of ROG Tg T cells (Fig 6).

Antigen-presenting cells used in *in vitro* stimulation and T_H1/T_H2 differentiation

Thy1.2-positive cells were eliminated from splenocytes with anti-Thy1.2 mAb (53-2.1) and magnetic bead sorting (MACS sorting, Mitenyi Biotec, Bergish Gladbach, Germany). Then Thy1.2-negative cells were irradiated (3500 rad) and used as antigen-presenting cells (APCs; 2×10^5; Figs 2, *A*; 4, *A*; 4, *B* and *C*; 5; and 9, *B*).

In vitro T_H1/T_H2 cell differentiation cultures

Naive ($CD44^{low}$) splenic DO11.10 Tg CD4 T cells (2×10^4) or OT-II Tg CD4 T cells (2×10^4) prepared by means of cell sorting were stimulated with indicated doses of antigenic OVA peptide (OVA 323-339) and irradiated (3500 rad) BALB/c or C57BL/6 APCs (Thy1.2-negative APCs, 2×10^5) in the presence of IL-2 (25 U/mL) and IL-4 (100 U/mL; T_H2 condition); IL-2 (25 U/mL), IL-12 (100 U/mL), and anti-IL-4 mAb (T_H1 condition); or IL-2 (25 U/mL) only (neutral condition).[E4]

In vitro ROG-overexpressing T_H2 cell cultures

Freshly isolated KJ1-positive CD4 T cells from DO11.10 Tg mice were stimulated with immobilized anti-TCR plus anti-CD28 mAb for 2 days. Then the *ROG* gene was introduced by using a retrovirus vector containing the *ROG-IRES-hNGFR* gene, and 4 days after infection, *hNGFR*-positive infected cells were enriched by sorting. Infected cells were stimulated with OVA peptide plus APCs in the presence of IL-2 for 5 days. Then the stimulated cells (1×10^6) were transferred into BALB/c *nu/nu* mice, as previously described.[E5]

Measurement of AHR

AHR responses were assessed by using methacholine-induced airflow obstruction in conscious mice placed in a whole-body plethysmograph (Buxco Electronics, Inc, Wilmington, NC), as described previously.[E6] Airway function was also assessed by measuring the changes in lung resistance and dynamic compliance in response to increasing doses of inhaled methacholine, as described previously.[E7,E8]

Analysis of lung histology

The lung samples taken on day 25 were sectioned and stained with H&E reagents, PAS reagents, and LUNA reagents, as previously described.[E6] PAS-positive cells were defined as the average of the score. The numeric scores for the abundance of PAS-positive mucus-containing cells in each airway were determined as follows: 0, less than 5% PAS-positive cells; 1, 5% to 25%; 2, 25% to 50%; 3, 50% to 75%; and 4, more than 75%.[E9]

Supplemental discussion

RANTES (CCL5) belongs to the CC chemokine family and induces leukocyte migration by binding to specific receptors in the G protein–coupled receptor family.[E10] RANTES is produced predominantly by CD8 T cells, epithelial cells, fibroblasts, and platelets and is associated with airways inflammation.[E11-E15] The modulation of RANTES expression by different levels of ROG was detected (Figs 2, *B*, and 4, *B*), whereas no difference was observed in the expression of RANTES in the transfer experiments by using BALB/c nude mice (Fig 5, *C*). The reason for this discrepancy remains unclear at this time, but this could be due to the absence of endogenous CD8 T cells in the host BALB/c *nu/nu* mice. A critical role of CD8 T cells in the OVA-induced airway inflammation has been reported.[E16] RANTES could be involved in the modulation of airway inflammation by CD8 T cells.

The absolute number of macrophages in the BAL fluid is enhanced after OVA challenge (Fig 1, *A*). No remarkable change in the number of macrophages between $ROG^{+/+}$ and $ROG^{-/-}$ mice was detected (Fig 1, *A*), and moderate decreases in the number of macrophages were observed in ROG Tg and in cell-transfer experiments with ROG-overexpressing cells (Fig 3, *A*; 5, *B*; and 6, *A*). Thus no clear link can exist between the expression levels of ROG and the level of infiltration of macrophages into the lung.

Kang et al[E17] demonstrate that $ROG^{-/-}$ T cells express more CD25 and CD69. We did not detect the difference in the expression of CD25 and CD69 in freshly prepared $ROG^{-/-}$ T cells (see Fig E1). Kang et al measured the expression of CD25 and CD69 after anti-TCR stimulation, whereas we examined the expression in freshly prepared CD4 T cells in Fig 1, *E*. Thus the apparent discrepancy between our results and theirs could be due to the cells analyzed in their studies compared with ours (activated vs not activated).

We showed a modulation effect of ROG Tg T cells in an OVA-induced airway inflammation model (Fig 6). The ROG-overexpressing cells showed the decreased ability to induce the airway inflammation (Fig 5). The expression levels of ROG in the retrovirus-transduced ROG-overexpressing T_H2 cells were modest compared with those of the ROG Tg T cells. Thus we performed the modulation experiment using ROG Tg T cells (Fig 6).

We measured the mRNA expression levels of TARC and MDC, which are known to be the chemokines for T_H cell recruitment, and no significant difference was noted in $ROG^{-/-}$ or ROG Tg mice compared with those in wild-type mice. It is known that macrophages, natural killer cells, and B cells constitutively secrete MDC,[E18] and TARC is secreted by airway epithelium.[E19] Thus ROG might not be involved directly in the regulation of the secretion of these chemokines.

REFERENCES

E1 Hogquist KA, Jameson SC, Heath WR, Howard JL, Bevan MJ, Carbone FR. T cell receptor antagonist peptides induce positive selection. Cell 1994;76:17-27.

E2 Barnden MJ, Allison J, Heath WR, Carbone FR. Defective TCR expression in transgenic mice constructed using cDNA-based α- and β-chain genes under the control of heterologous regulatory elements. Immunol Cell Biol 1998;76:34-40.

E3 Murphy KM, Heimberger AB, Loh DY. Induction by antigen of intrathymic apoptosis of $CD4^+CD8^+TCR^{lo}$ thymocytes in vivo. Science 1990;250:1720-3.

E4 Yamashita M, Kimura M, Kubo M, Shimizu C, Tada T, Perlmutter RM, et al. T cell antigen receptor-mediated activation of the Ras/mitogen-activated protein kinase pathway controls interleukin 4 receptor function and type-2 helper T cell differentiation. Proc Natl Acad Sci U S A 1999;96:1024-9.

E5 Yamashita M, Hirahara K, Shinnakasu R, Hosokawa H, Norikane S, Kimura MY, et al. Crucial role of MLL for the maintenance of memory T helper type 2 cell responses. Immunity 2006;24:611-22.

E6 Kamata T, Yamashita M, Kimura M, Murata K, Inami M, Shimizu C, et al. src homology 2 domain-containing tyrosine phosphatase SHP-1 controls the development of allergic airway inflammation. J Clin Invest 2003;111:109-19.

E7 Takeda K, Hamelmann E, Joetham A, Shultz LD, Larsen GL, Irvin CG, et al. Development of eosinophilic airway inflammation and airway hyperresponsiveness in mast cell-deficient mice. J Exp Med 1997;186:449-54.

E8 Koya T, Kodama T, Takeda K, Miyahara N, Yang ES, Taube C, et al. Importance of myeloid dendritic cells in persistent airway disease after repeated allergen exposure. Am J Respir Crit Care Med 2006;173:42-55.

E9 Myou S, Leff AR, Myo S, Boetticher E, Tong J, Meliton AY, et al. Blockade of inflammation and airway hyperresponsiveness in immune-sensitized mice by dominant-negative phosphoinositide 3-kinase-TAT. J Exp Med 2003;198:1573-82.

E10 Zlotnik A, Yoshie O. Chemokines: a new classification system and their role in immunity. Immunity 2000;12:121-7.

E11 Kameyoshi Y, Dorschner A, Mallet AI, Christophers E, Schroder JM. Cytokine RANTES released by thrombin-stimulated platelets is a potent attractant for human eosinophils. J Exp Med 1992;176:587-92.

E12 Olszewska-Pazdrak B, Casola A, Saito T, Alam R, Crowe SE, Mei F, et al. Cell-specific expression of RANTES, MCP-1, and MIP-1alpha by lower airway epithelial cells and eosinophils infected with respiratory syncytial virus. J Virol 1998;72:4756-64.

E13 Matsukura S, Kokubu F, Kubo H, Tomita T, Tokunaga H, Kadokura M, et al. Expression of RANTES by normal airway epithelial cells after influenza virus A infection. Am J Respir Cell Mol Biol 1998;18:255-64.

E14 Schall TJ, Jongstra J, Dyer BJ, Jorgensen J, Clayberger C, Davis MM, et al. A human T cell-specific molecule is a member of a new gene family. J Immunol 1988;141:1018-25.

E15 Oliva A, Kinter AL, Vaccarezza M, Rubbert A, Catanzaro A, Moir S, et al. Natural killer cells from human immunodeficiency virus (HIV)-infected individuals are an important source of CC-chemokines and suppress HIV-1 entry and replication in vitro. J Clin Invest 1998;102:223-31.

E16 Miyahara N, Swanson BJ, Takeda K, Taube C, Miyahara S, Kodama T, et al. Effector CD8+ T cells mediate inflammation and airway hyper-responsiveness. Nat Med 2004;10:865-9.

E17 Kang BY, Miaw SC, Ho IC. ROG negatively regulates T-cell activation but is dispensable for Th-cell differentiation. Mol Cell Biol 2005;25: 554-62.

E18 Andrew DP, Chang MS, McNinch J, Wathen ST, Rihanek M, Tseng J, et al. STCP-1 (MDC) CC chemokine acts specifically on chronically activated Th2 lymphocytes and is produced by monocytes on stimulation with Th2 cytokines IL-4 and IL-13. J Immunol 1998;161:5027-38.

E19 Heijink IH, Marcel Kies P, van Oosterhout AJ, Postma DS, Kauffman HF, Vellenga E. Der p, IL-4, and TGF-beta cooperatively induce EGFR-dependent TARC expression in airway epithelium. Am J Respir Cell Mol Biol 2007; 36:351-9.